Conventional applications of Thin Films

Jari Koskinen

Hardness, protection and wear

Diamond-like carbon

Art & Decoration

Titanium Nitride,
Titanium Dioxide

Applications of thin films

- Electronic components
  - semiconducting, dielectric, insulating, conductors, barriers…
- Hard protective coatings
  - Tribology short
  - Cutting tools: metal
  - Metal forming
  - Componets
    - Combustion engine
    - Turbine blades
- Decorative films
  - Metal
  - Interference coatings
  - Pagaging,
- Decorative and wear-resistant (decorative/functional) coatings
  - TiN
- Permeation barriers for moisture and gases
  - Bottle
  - Pacaging (Aluminium)
- Corrosion resistant films
  - ALD
- Dry film solid lubricants
  - DLC, MoS2

Coatings tribology

Adhesion – interfacial toughness

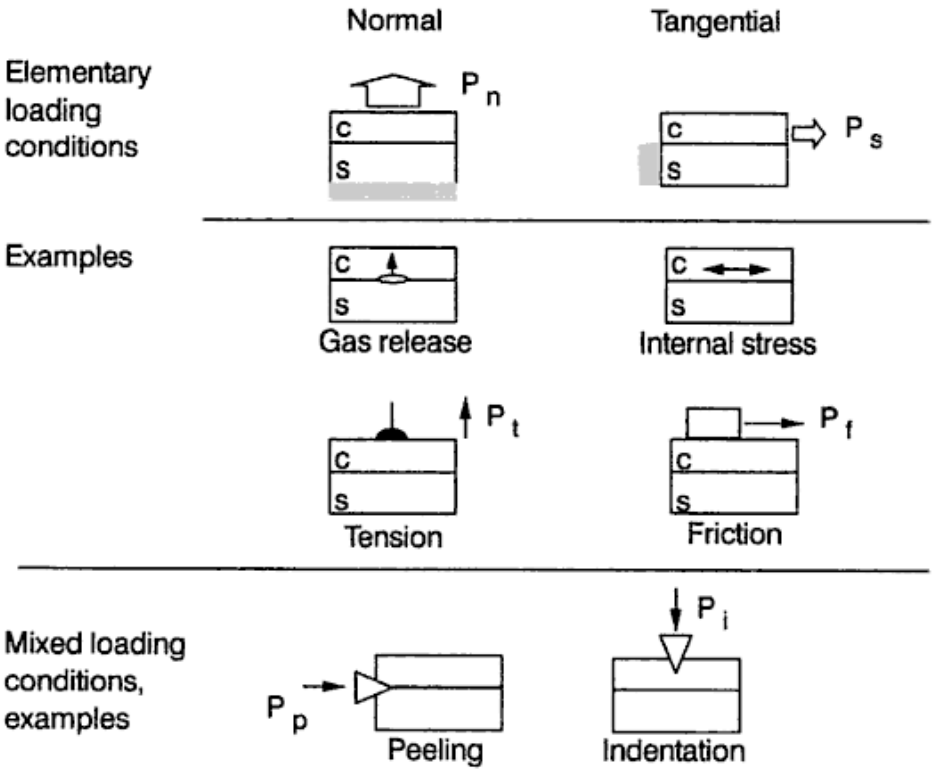

Figure 1. Loading conditions of coating-substrate systems. *c:* coating; *s:* substrate; P_n: normal force; P_s: shear force; P_t: tension force; P_f : friction force; P_p: peel force; P_i: indentation force.

Scratch testing

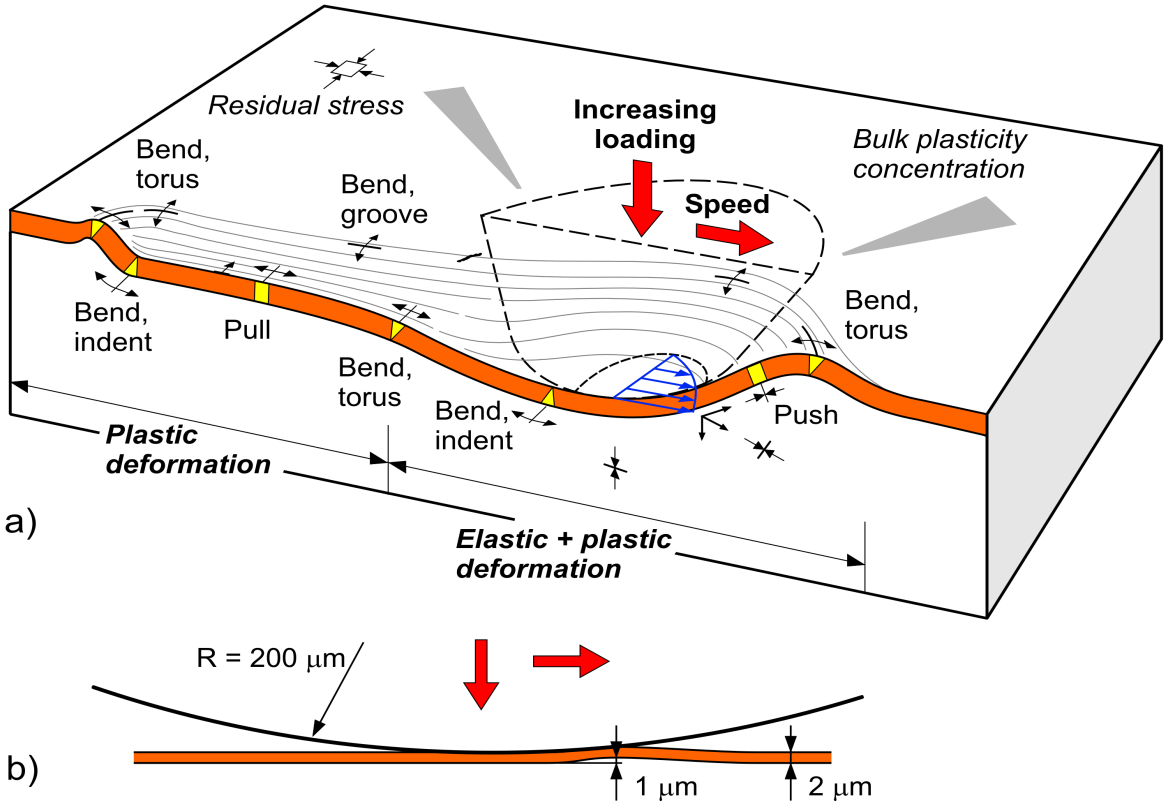

Scratch testing

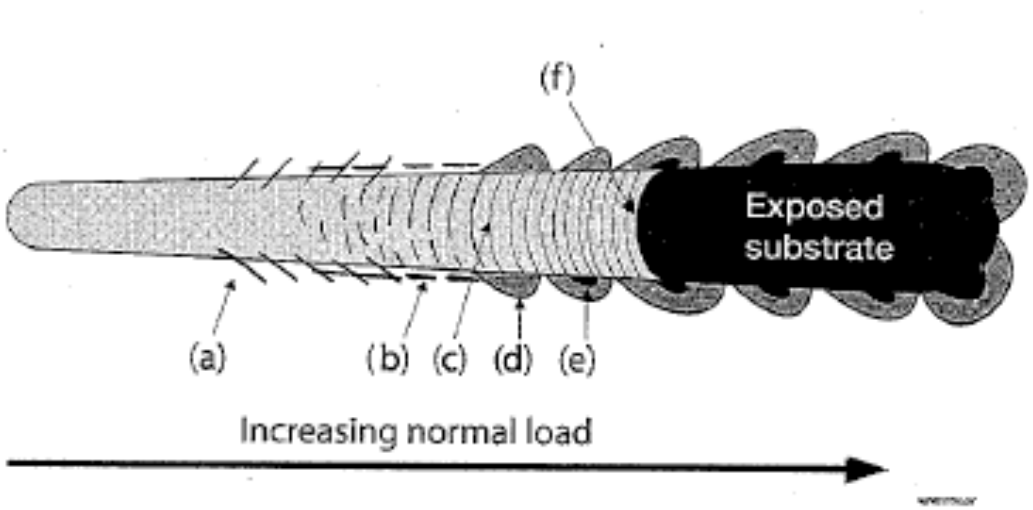

Fig. 3.61. The surface cracks generated in a scratch test track can be classified as (a) angular cracks, (b) parallel cracks, (c) transverse semicircular cracks, (d) coating chipping, (e) coating spalling and (f) coating breakthrough (modified after Larsson *et al.*, 1996).

- **Critical load L_c**
- **A value related to adhesion strength**
- **Modelling FEM: Fracture toughness K_c**

Examples

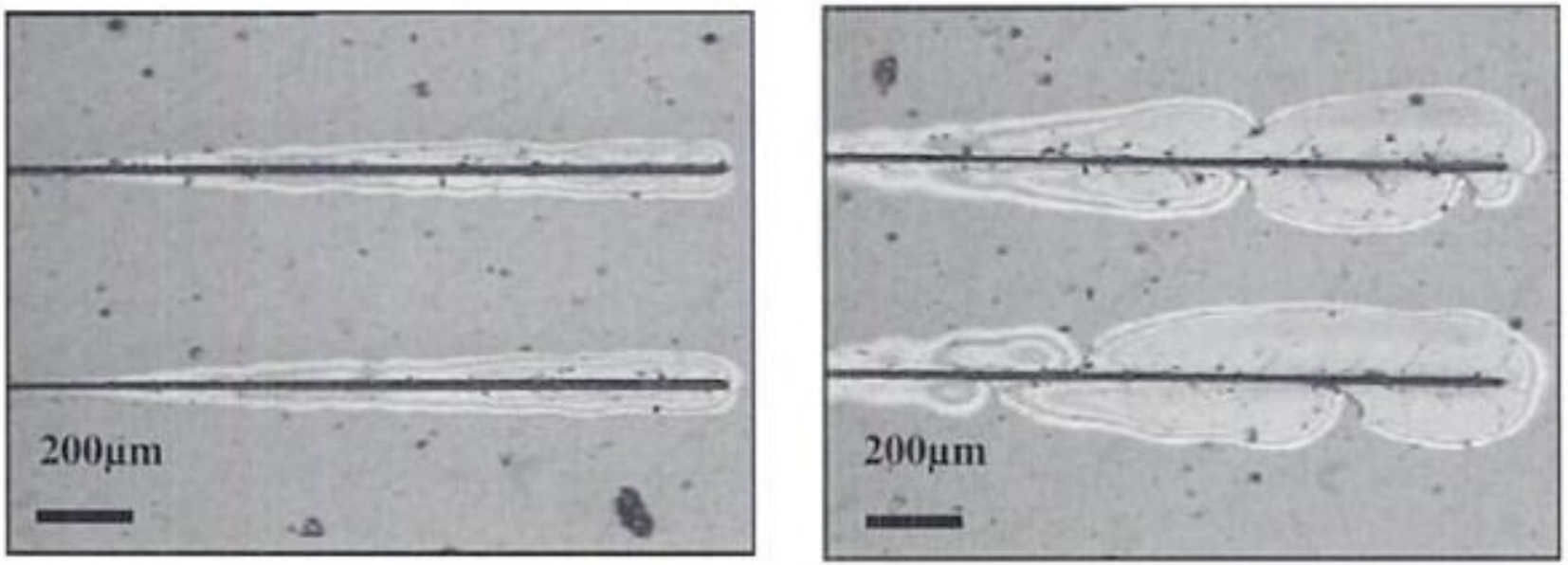

Figure 7. A comparison of two TiO_2 coated glass substrates subjected to a progressive normal load scratch of 0-50 mN with a 10 µm diamond indenter. The scratch speed is 2.5 mm/minute at a length of 2.5 mm. The sample on the left was classified as high roughness while the one on the right is classified as exhibiting low roughness.

Acoustic signal scratch testing

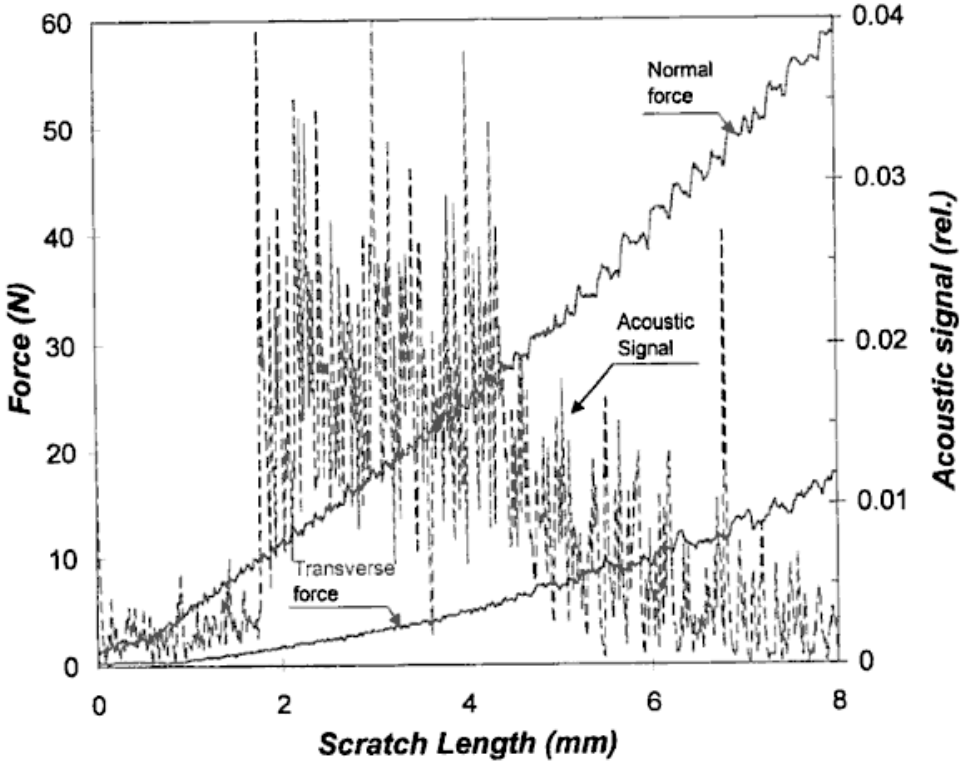

Figure 2. Plots for a scratch test performed on a sample of 3.12 μm thick nanophase diamond on a 304 stainless steel substrate. Normal scratch load, transverse force and acoustic emission plots are given as a function of scratch length.

FEM modeling of stresses in scratch test

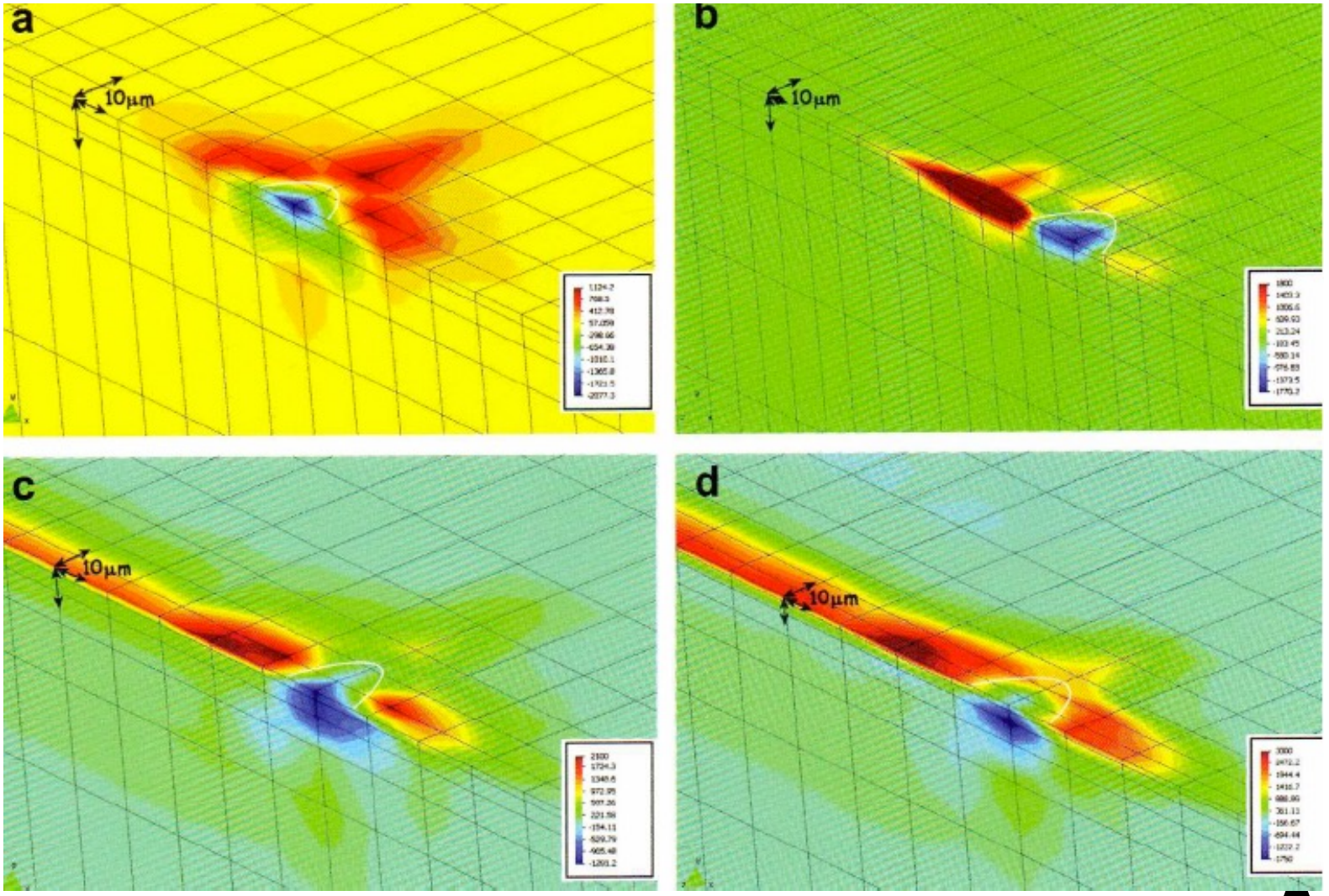

K. Holmberg et al. Coatings Tribology, 2009)

Rockwell indentation adhesion test

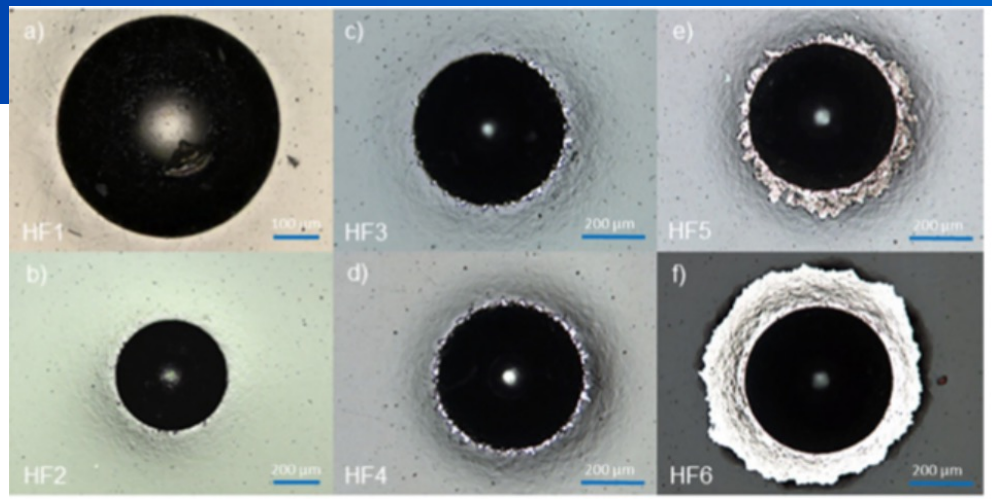

https://www.oerlikon.com/balzers/com

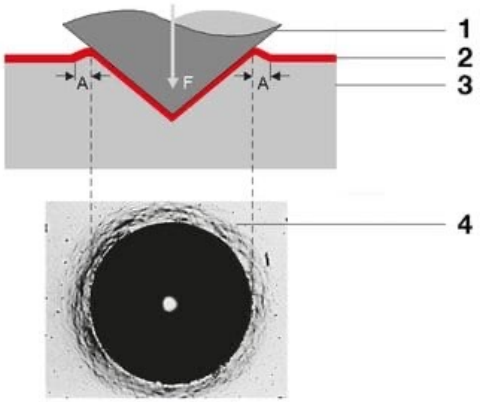

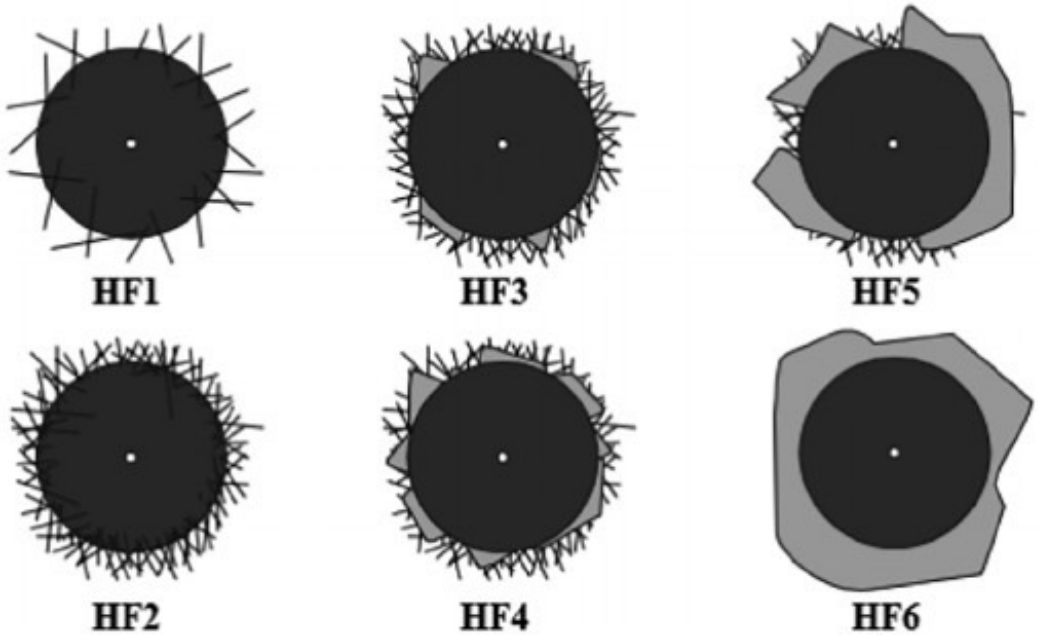

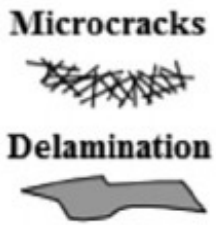

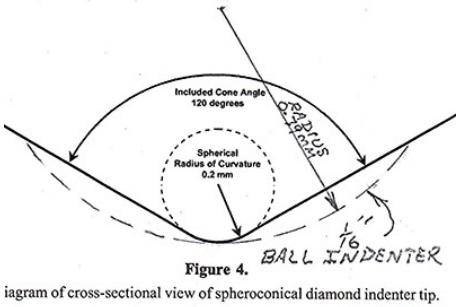

Figure 4.

iagram of cross-sectional view of spheroconical diamond indenter tip.

https://doi.org/10.1016/j.surfcoat.2020.125365

Parameters influencing friction and wear

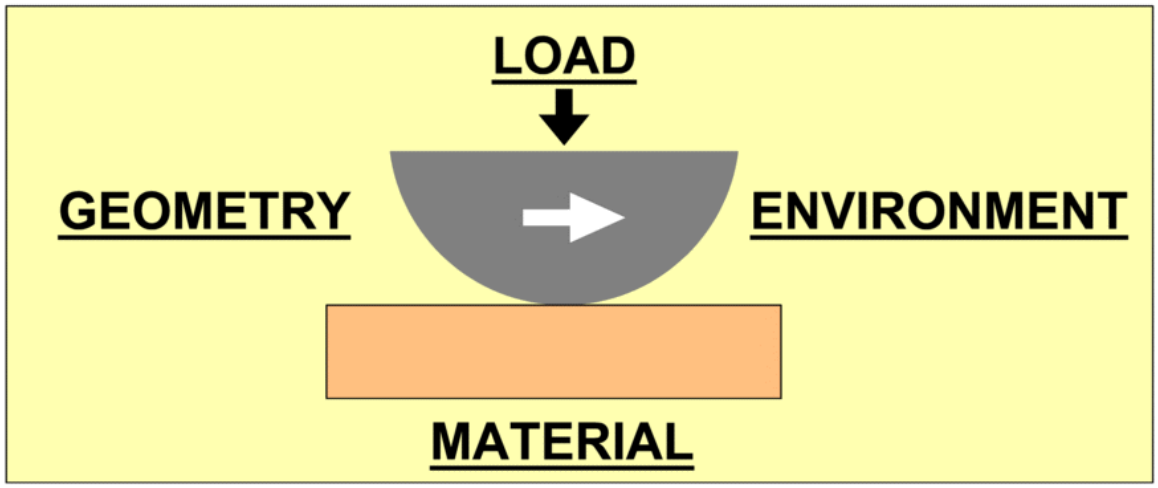

kgh1.dsf

GEOMETRY

- Macrogeometry
- Topography
- Debris
- Transfer layers
- Coating thickness

LOAD

- Normal load
- Tangential load

→ Speed

ENVIRONMENT

- Temperature
- Humidity
- Gas, liquid
- Radiation

MATERIAL

- Elasticity
- Plasticity
- Fracture toughness
- Chemical reactivity

kghcf1.dsf

Features of a (metal) surface in contact

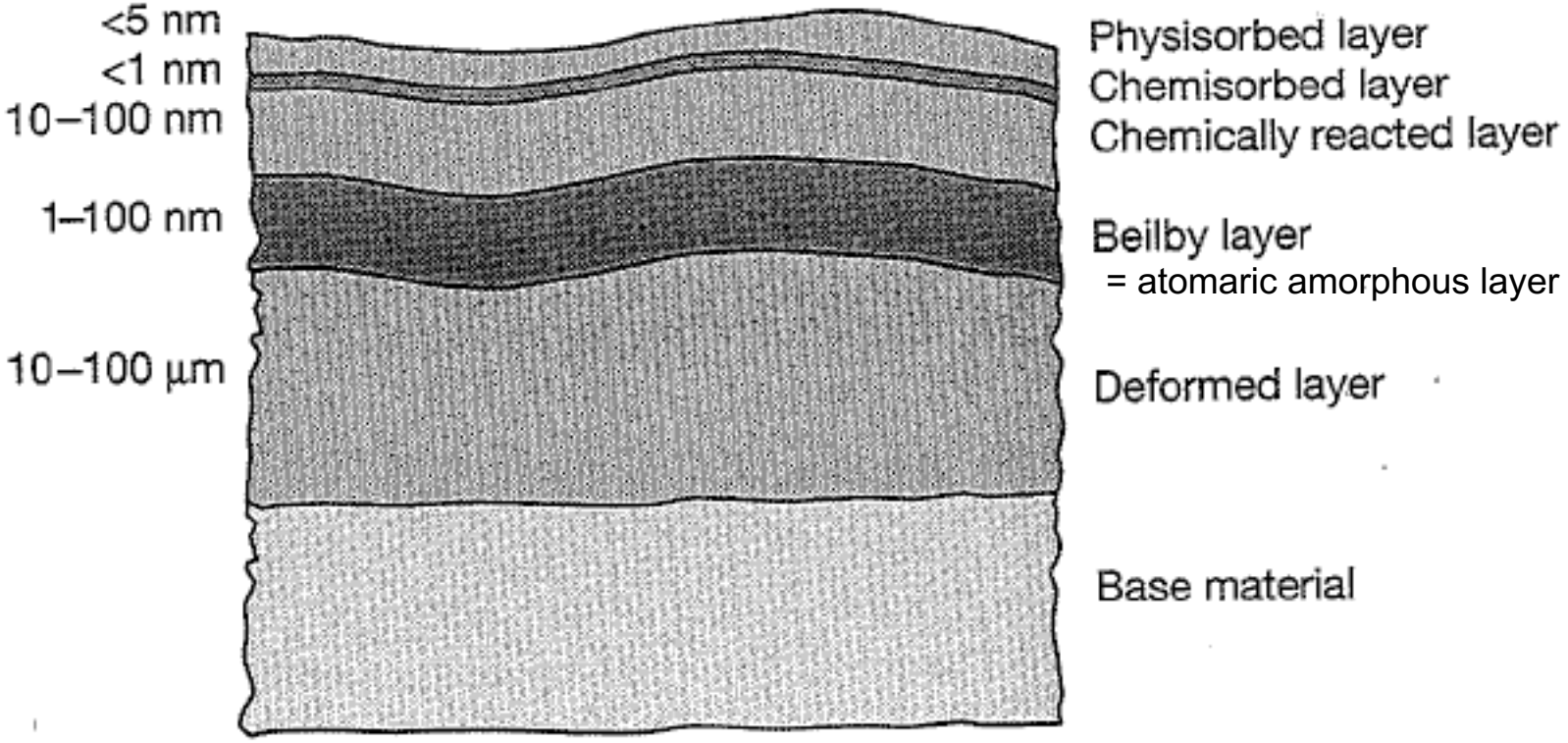

Sizes ranges

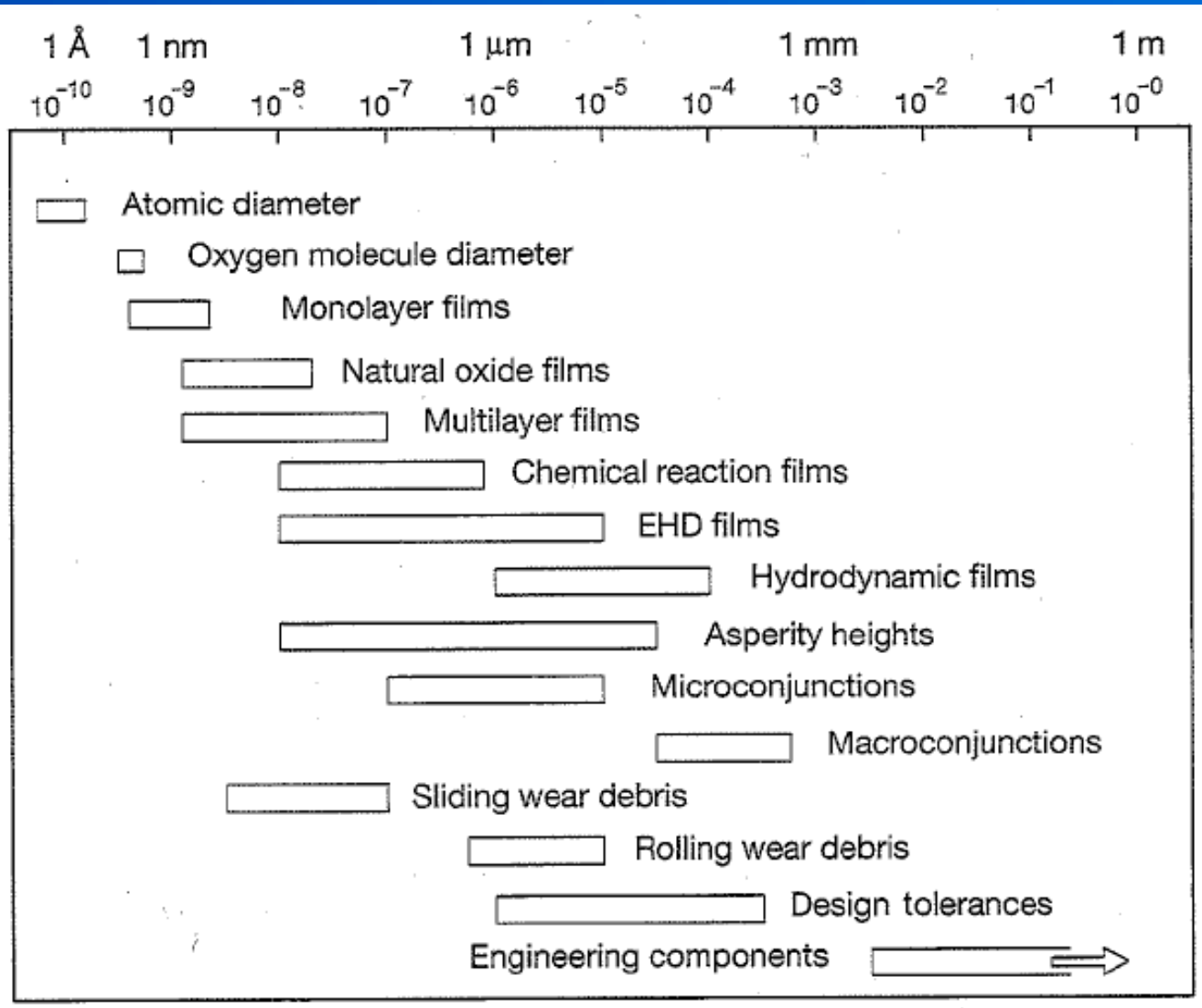

Fig. 3.5. Sizes of surface elements and surface-related phenomena.

Processes from loading to wear

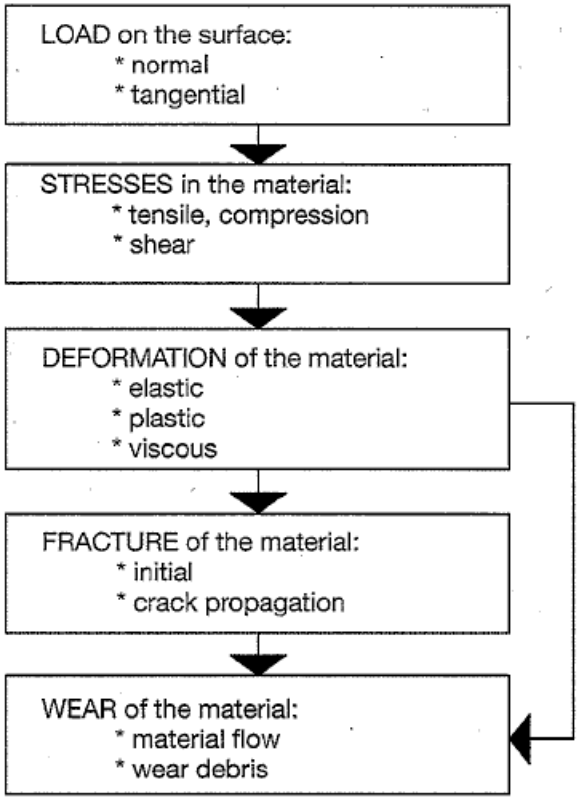

Fig. 3.25. Schematic diagram of the process from loading of the surface to wear.

Wear

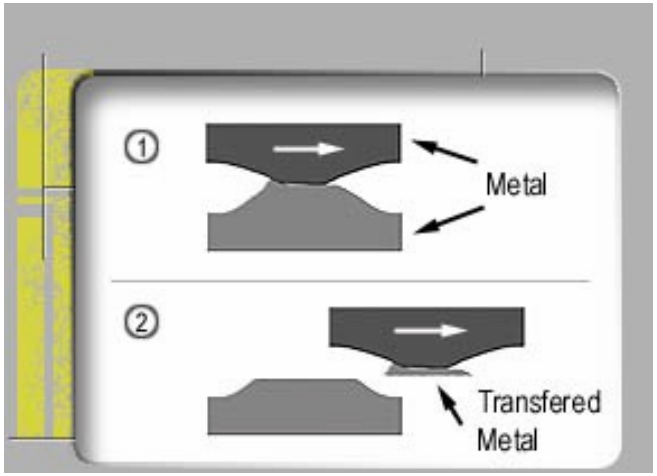

Adhesive

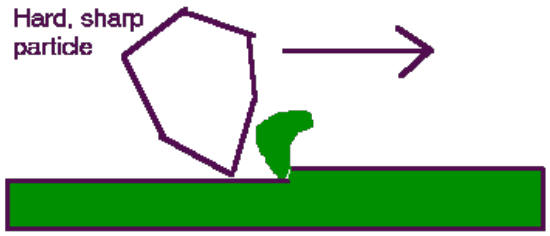

Abrasive

$$V = K\frac{w \bullet s}{H}$$

by Holm and Archard
V wear volume
w normal load
s sliding distance
H hardness

Plastic deformation in wear – example of Au films

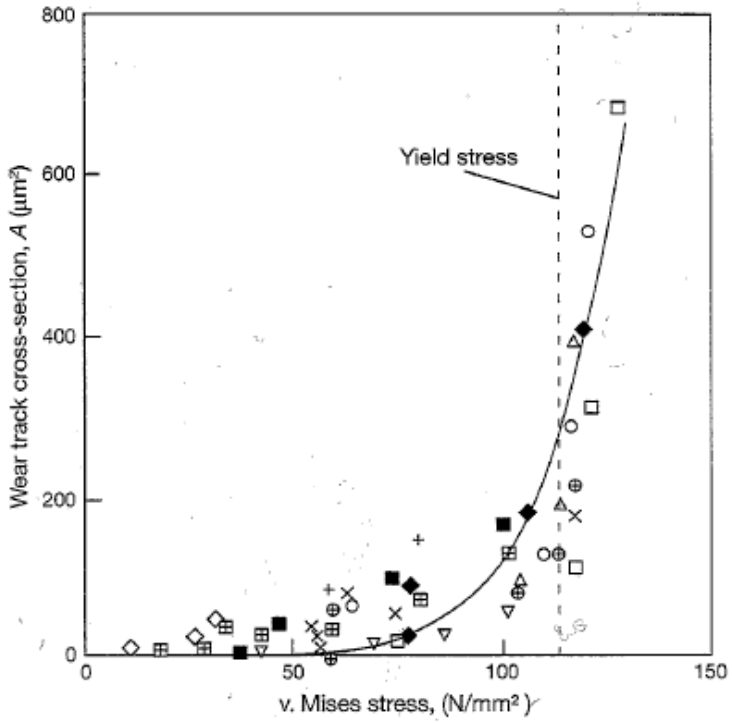

85. Cross-section of the wear track for both evaporated and electrodeposited gold layers as ion of the von Mises stress averaged over the depth and the contact radius for 56 different contact ns. The solid line is obtained from a wear model (data from Tangena, 1989).

Wear

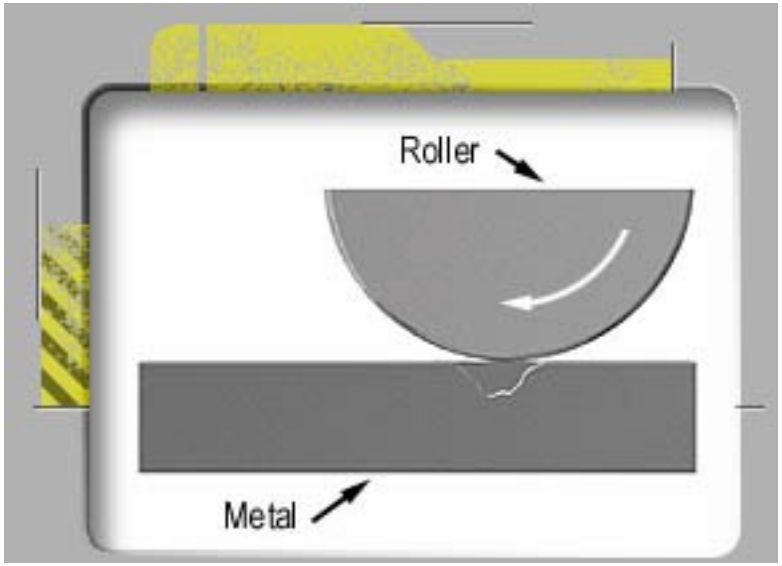

fatique

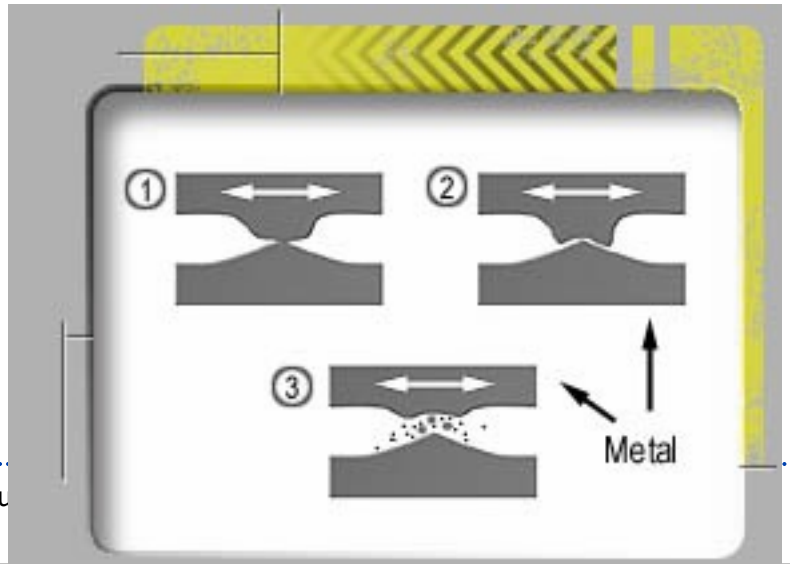

Fretting

Some coating wear modes

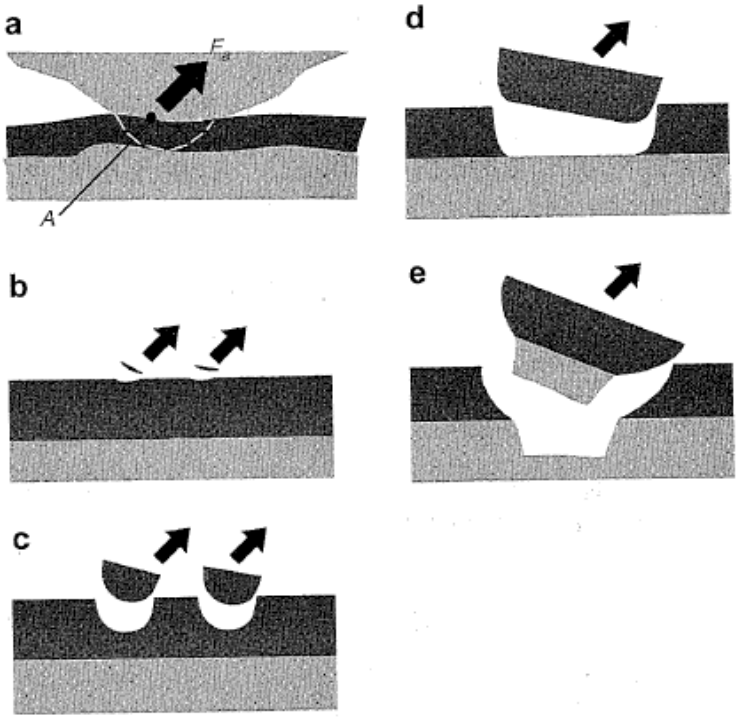

Fig. 3.97. Two surfaces attach to each other by adhesion (a) and the movement of the top surface results in an adhesive force, F_a, that tries to detach material over an area, A, from one of the surfaces. The detachment may take place (b) at the top surface, (c) within the coating, (d) at the coating/substrate interface and (e) in the substrate.

Coating interface at indentation

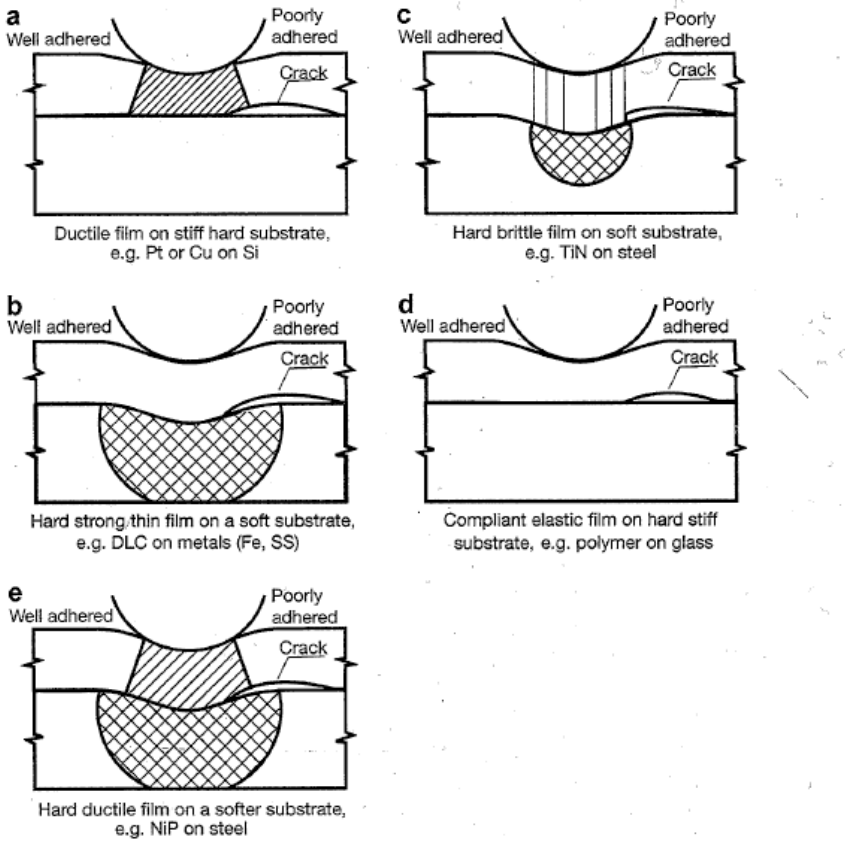

Fig. 3.62. Schematic cross-sections of various coating–substrate materials combinations and the influence of interfacial adhesion on cracking in indentation (after Swain and Mencik, 1994).

Stress countours, normaized to von Mises stresses (≈ σ_y)

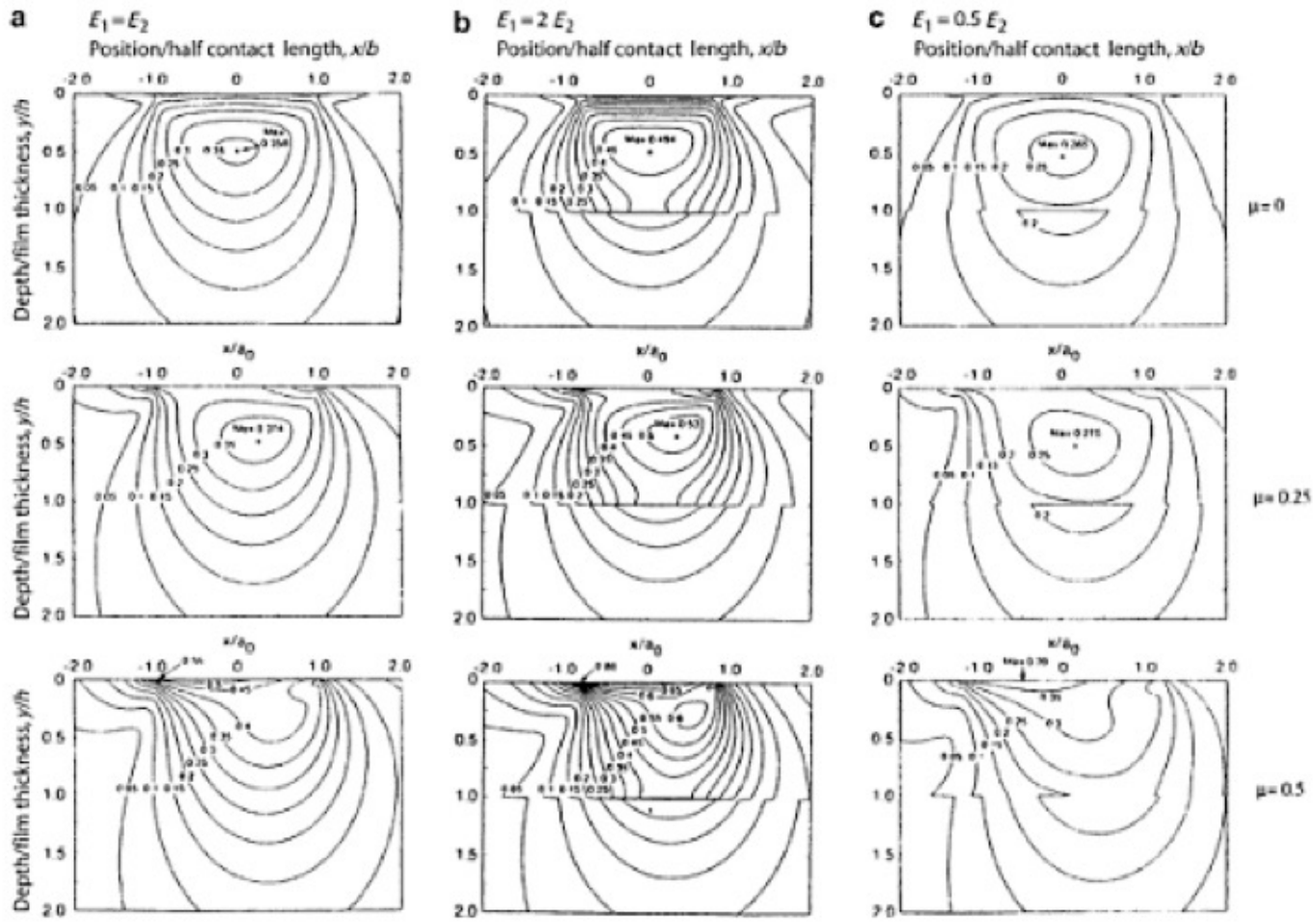

Fig. 3.33. Contour plots of normalized von Mises stresses, σ'/p_{max}, in the surface layer (E_1) and the substrate (E_2) with (a) no surface layer, $E_1 = E_2$, (b) a stiff layer, $E_1 = 2E_2$, and (c) an elastic layer, $E_1 = 0.5E_2$, when loaded by a sliding rigid *spherical* countersurface with coefficients of friction of $\mu = 0$, 0.25 and 0.5 (after O'Sullivan and King, 1988).

Multilayer with gradient

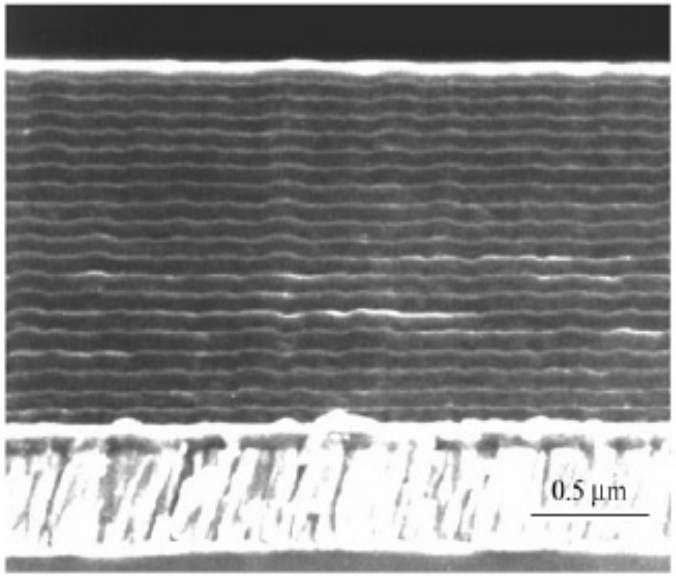

(b)

Fig. 6 A multilayer coating with multiple Ti/DLC pairs on top of a functionally gradient layer for an optimum combination of cohesive and adhesive toughness: (a) design schematic; (b) cross sectional photograph of the coating produced with 20 Ti/DLC pairs[18].

Material	Hardness	Elastic modulus	Thickness
DLC at 10^{-5} Pa	70 GPa	650 GPa	400 nm
DLC at 2×10^{-1} Pa	43 GPa	450 GPa	100 nm
$Ti_{0.10}C_{0.90}$	25 GPa	290 GPa	25 nm
$Ti_{0.25}C_{0.75}$	27 GPa	350 GPa	25 nm
$Ti_{0.30}C_{0.70}$	29 GPa	370 GPa	100 nm
$Ti_{0.50}C_{0.50}$	20 GPa	290 GPa	100 nm
$Ti_{0.70}C_{0.30}$	14 GPa	230 GPa	100 nm
$Ti_{0.90}C_{0.10}$	6 GPa	150 GPa	50 nm
α-Ti	4 GPa	140 GPa	50 nm
440C steel	11 GPa	220 GPa	

 Tsinghua Science and Technology, December 2005, 10(6): 665-679

Tribological properties

- **Friction and wear performance evaluated:**
  - pin-on-disc
  - reciprocative test
  - unlubricated in normal atmosphere
  - unlubricated in dry air
  - lubricated with water and lubricating oil

Improved tribological properties of components by surface coatings

Reduced friction

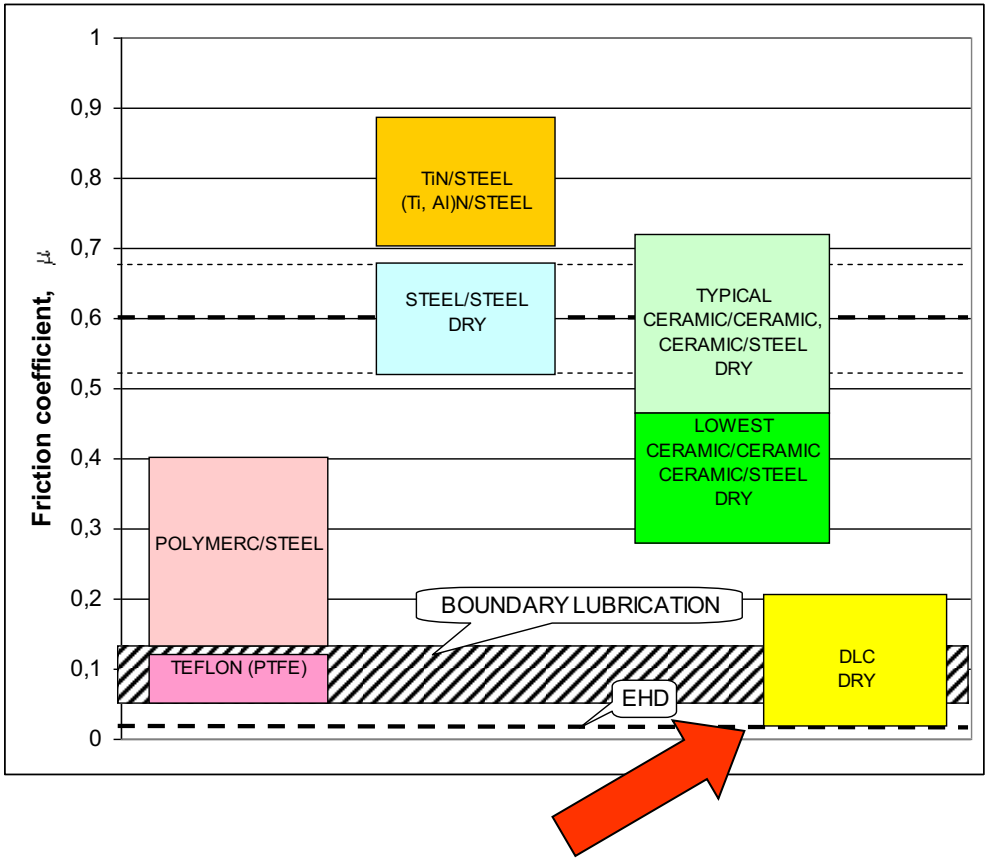

Increased wear resistance

Cutting tool coatings

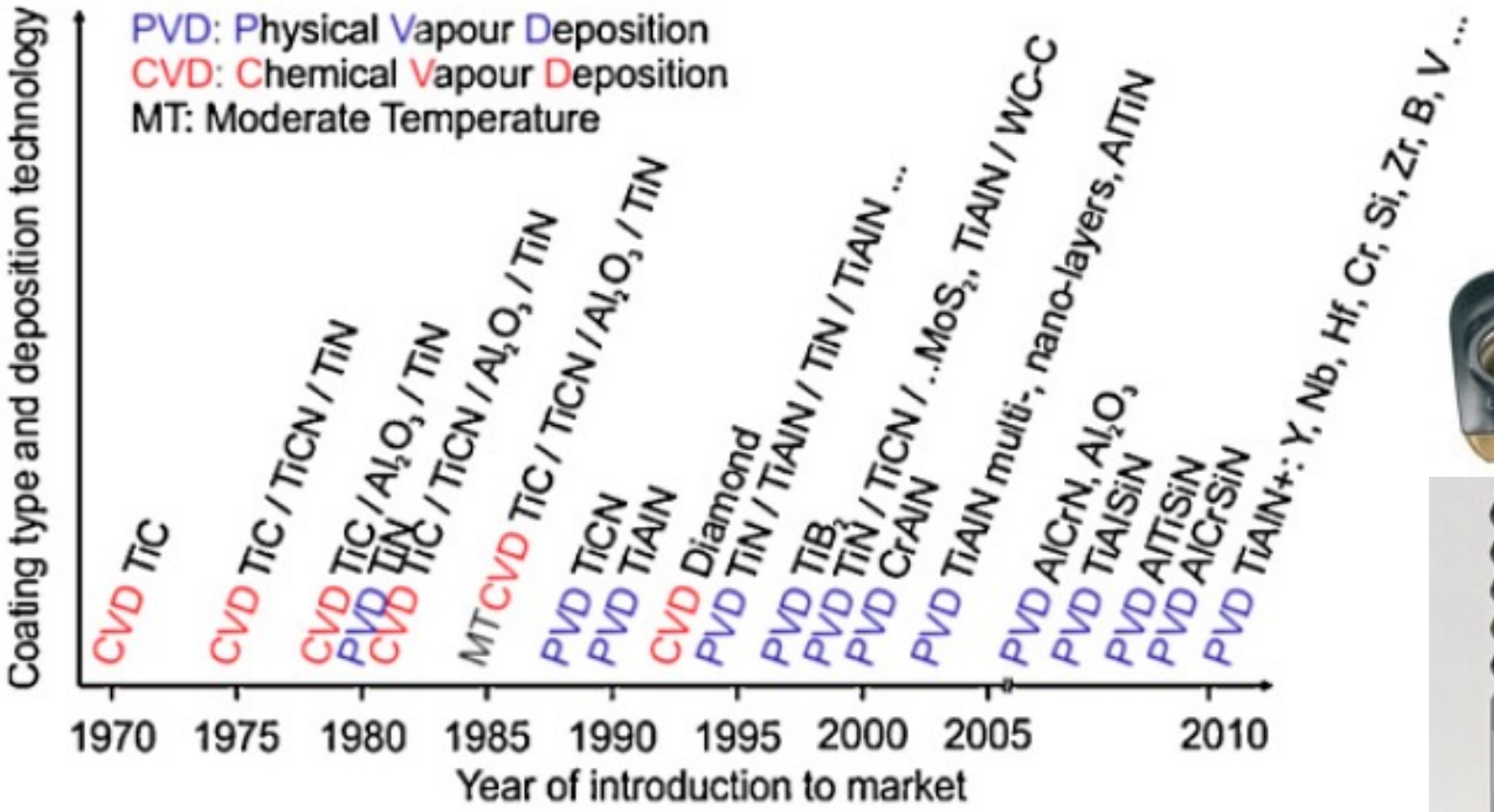

Fig. 7. Evolution of coating materials for cutting tools

K.-D. Bouzakis et al./CIRP Annals - Manufacturing Technology 61 (2012) 703–723

TiAlN

- Titanium aluminium nitride (TiAlN) or aluminium titanium nitride (AlTiN; for aluminium contents higher 50 at.%) stands for a group of metastable hard coatings consisting of the metallic elements aluminium and titanium, and nitrogen.
- Why TiAlN coatings outperform pure Titanium nitride (TiN):
- Increased oxidation resistance at elevated temperatures due to the formation of a protective aluminium-oxide layer at the surface
- Increased hardness in the freshly deposited films due to micro-structure changes and solid solution hardening
- Age hardening of the coatings at temperatures typical for cutting tools operation due to spinodal decomposition of TiAlN into TiN and cubic AlN

From WIKI

Tool coating process

Metal turing tool

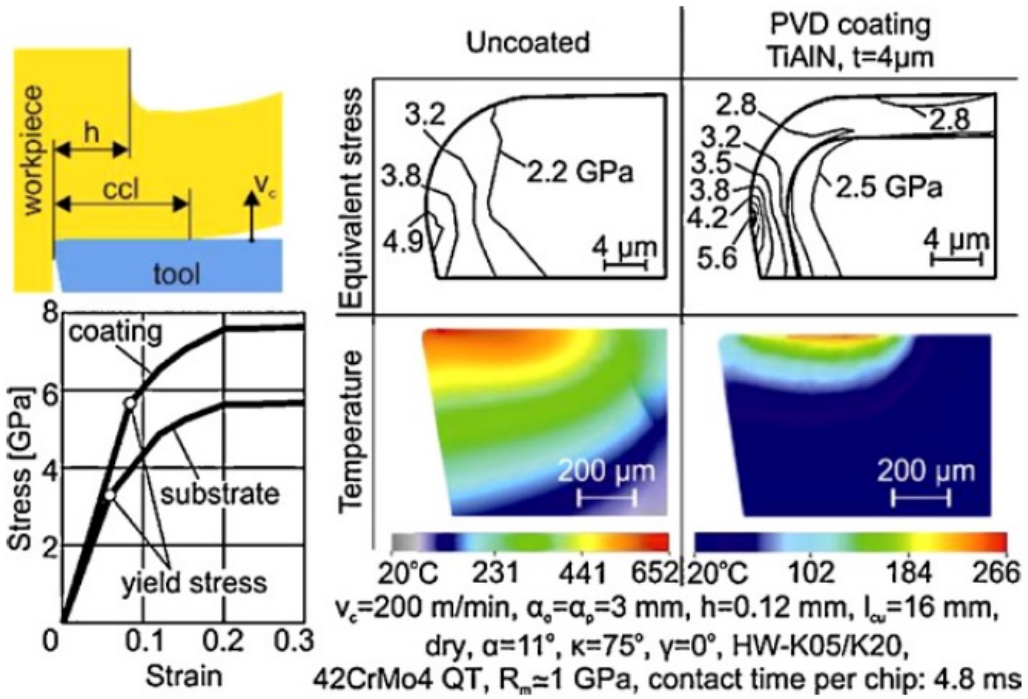

Fig. 1. Decrease of mechanical and thermal loads of cemented carbide tools in milling by the application of PVD-coatings.

HIPIMS TiAlN

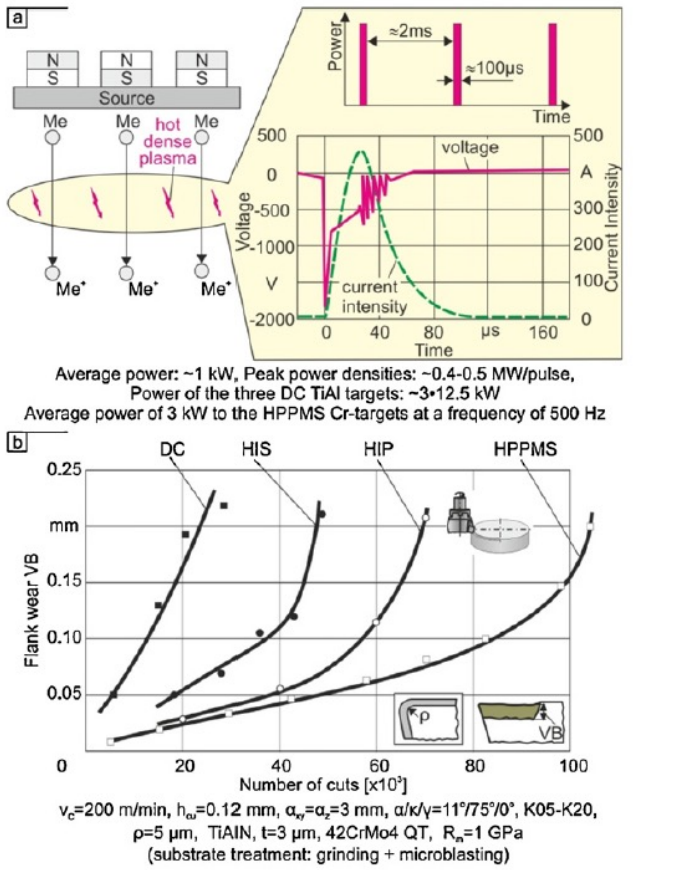

Fig. 3. (a) Plasma energy increase by HPPMS and (b) effect of PVD deposition process on cutting performance for a typical (Ti,Al)N film.

CrAlSiN coating

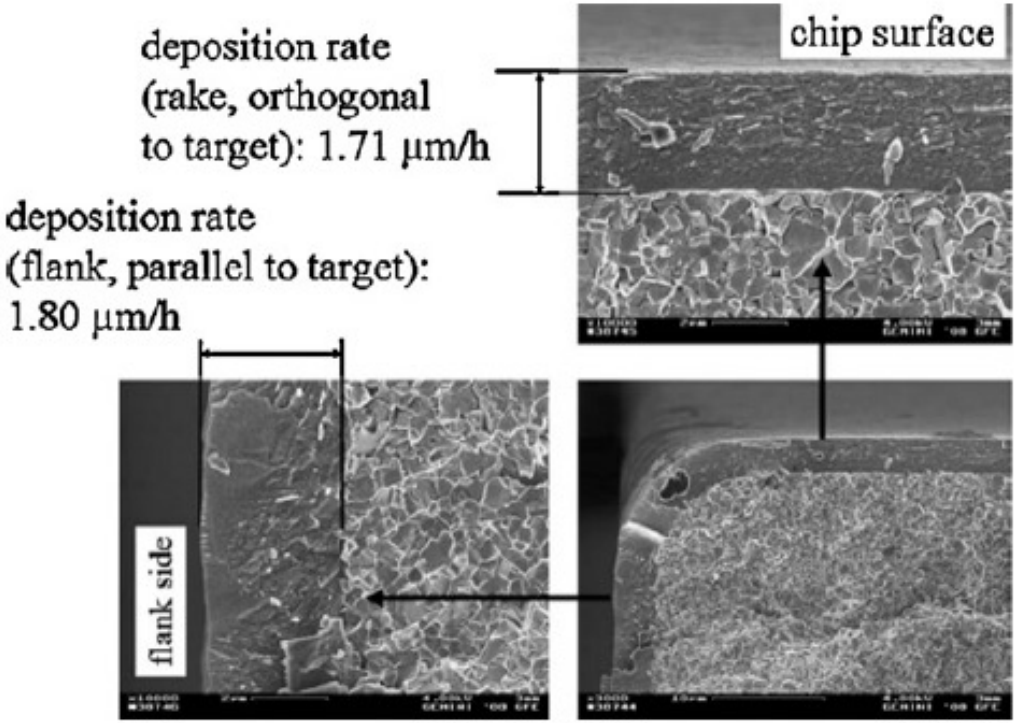

Fig. 4. SEM micrographs of cross sections from $(Cr_{0.5}Al_{0.45}Si_{0.05})N$ grown by HPPMS showing a high thickness uniformity around the cutting edge [14].

Coated Tool Information

AlTiN TiN TiCN nACo nACRo ZrN CVD Diamond PVD Diamond

		1st Digit of Coated EDP	Hardness	Thermal Stability
TiN	Titanium Nitride	2	24GPa	1112F (600C)
TiCN	Titanium Carbonitride	4	37GPa	752F (400C)
AlTiN	Aluminum Titanium Nitride	5	38GPa	1472F (800C)
nACo	Aluminum Titanium Nitride + Silicon Nitride	8	45GPa	2192F (1200C)
nACRo	Aluminum Chrome Nitride + Silicon Nitride	-	40GPa	2012F (1100C)
ZrN	Zirconium Nitride	6	25GPa	1049F (565C)
DIA	CVD Diamond	-	80-100GPa	1094F (590C)
DLC	PVD Diamond	-	70-90GPa	932F (500C)

http://www.endmill.com/pages/coatings.html

Coating selection

Material	Hardness	TiN	TiCN	AlTiN	nACo	nACRo	ZrN	DIA
Austenitic Stainless Steel	< 35 HRc	*	X		*			
Martinsitic Stainless Steel	< 35 HRc	*	*	*	X			
Martinsitic Stainless Steel	>= 35 HRc			*	X			
PH Stainless Steel	< 35 HRc	*		*	X			
PH Stainless Steel	>= 35 HRc			*	X			
Ni, Co, Fe Based Super Alloys				*	X	X_1		
Titanium				*	X	X_1		
Alloy Steel	16-23 HRc	*	*	X				
Alloy Steel	23-38 HRc	*	*	X	*			
Alloy Steel	> 38 HRc			*	X			
Carbon Steel	16-23 HRc	*	*	X				
Carbon Steel	23-38 HRc	*	*	X	*			
Carbon Steel	> 38 HRc			*	X			
Low Carbon Steel	13-23 HRc	*	*	X				
Low Carbon Steel	23-38 HRc	*	*	X	*			
Low Carbon Steel	> 38 HRc			*	X			
Gray Cast Iron	18-22 HRc		*	*	X			
Nodular Cast Iron	22-32 HRc	*	X		*			
Aluminium <10% Si			*				X	
Aluminium >10% Si						*		X
Graphite								X
Composits								X
Hardened Steel	>45 HRc				X			

X = For BEST performance
X_1 = For SPECIFIC applications
* = Additional recommended coating options

http://www.endmill.com/pages/coatings.html

Coating selection Hauzer

Tool Coatings	*Deposition Temperature Range °C*	*Maximum Operating Temperature °C*
TiN	<600	600
AlTiN	<600	900
AlTiN + W: C-H	150-450	450
AlTiN + Al_2O_3	450-600	1100
AlCrN	<600	1100
TiSiN	<600	1500
TiCN	<600	600
TiAlN	<600	800
TiN + TiAlN multilayer	<600	800
CrCN	450	600
ta-C	80-200	>500

Table 1. *An overview of tool coatings and their maximum temperatures.*

continued on page 44

Coated components for wear and friction - automotive

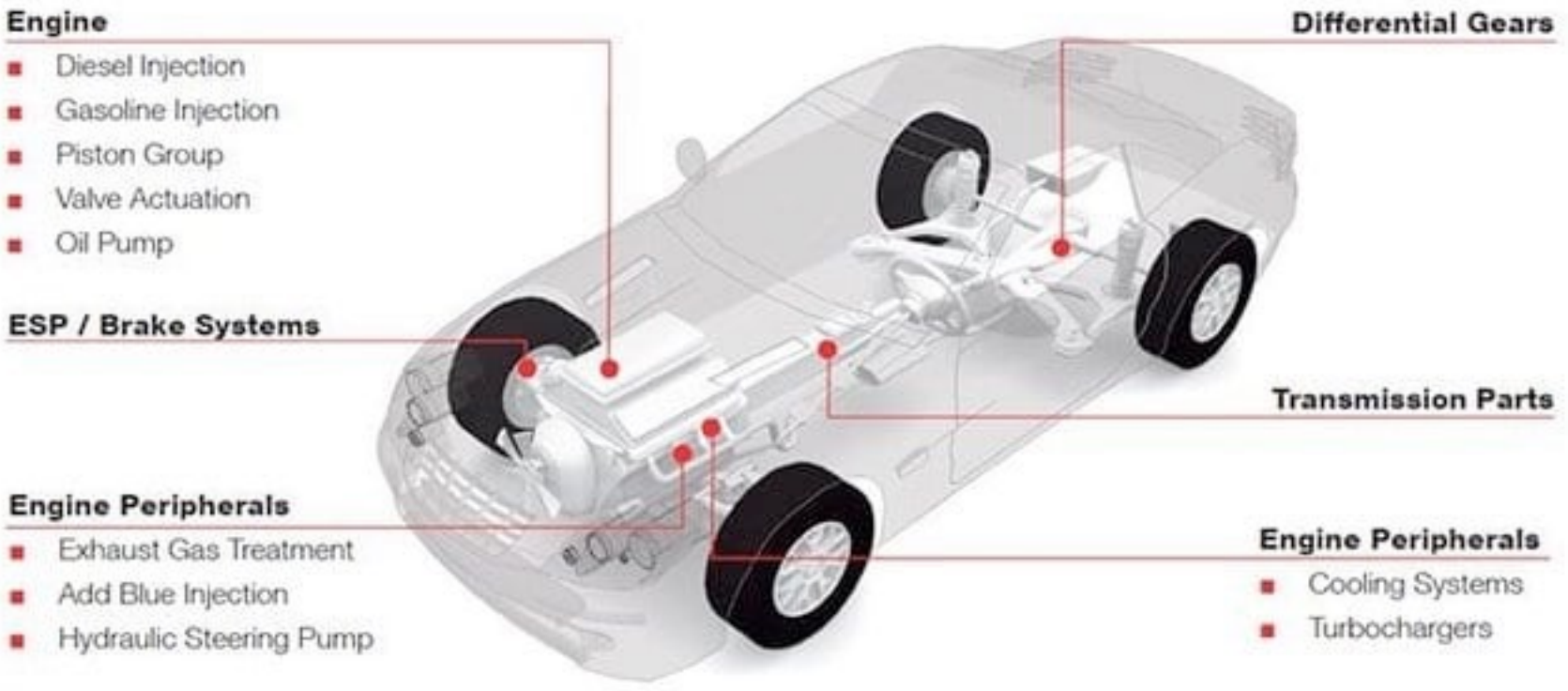

https://www.oerlikon.com/balzers/sg/en/markets/automotive-and-transportation/automotive/automotive-components/

Coated components for wear and friction – automotive Hauzer

Technology	*Arc Evaporation (PVD)*	*Sputtering (PVD)*	*High Voltage Discharge (PACVD)*
Typical Coatings	CrN, ta-C	CrN, metal DLC, ASIN	DLC, Silicon DLC
Surface	Rough (polish)	Smooth	Smooth
Typical Applications	Valve train components, diesel high pressure pump, diesel injector parts, piston rings	Valve train components, journal bearings	Piston parts, valve train components, diesel injector parts, diesel high pressure and oil pump parts, piston pins, gears

Table 2. *Technology, coatings and the engine components for which they are mainly used.*

Motor

DLC

Energy consumption of a car

K. Holmberg et al. / Tribology International 47 (2012) 221–234

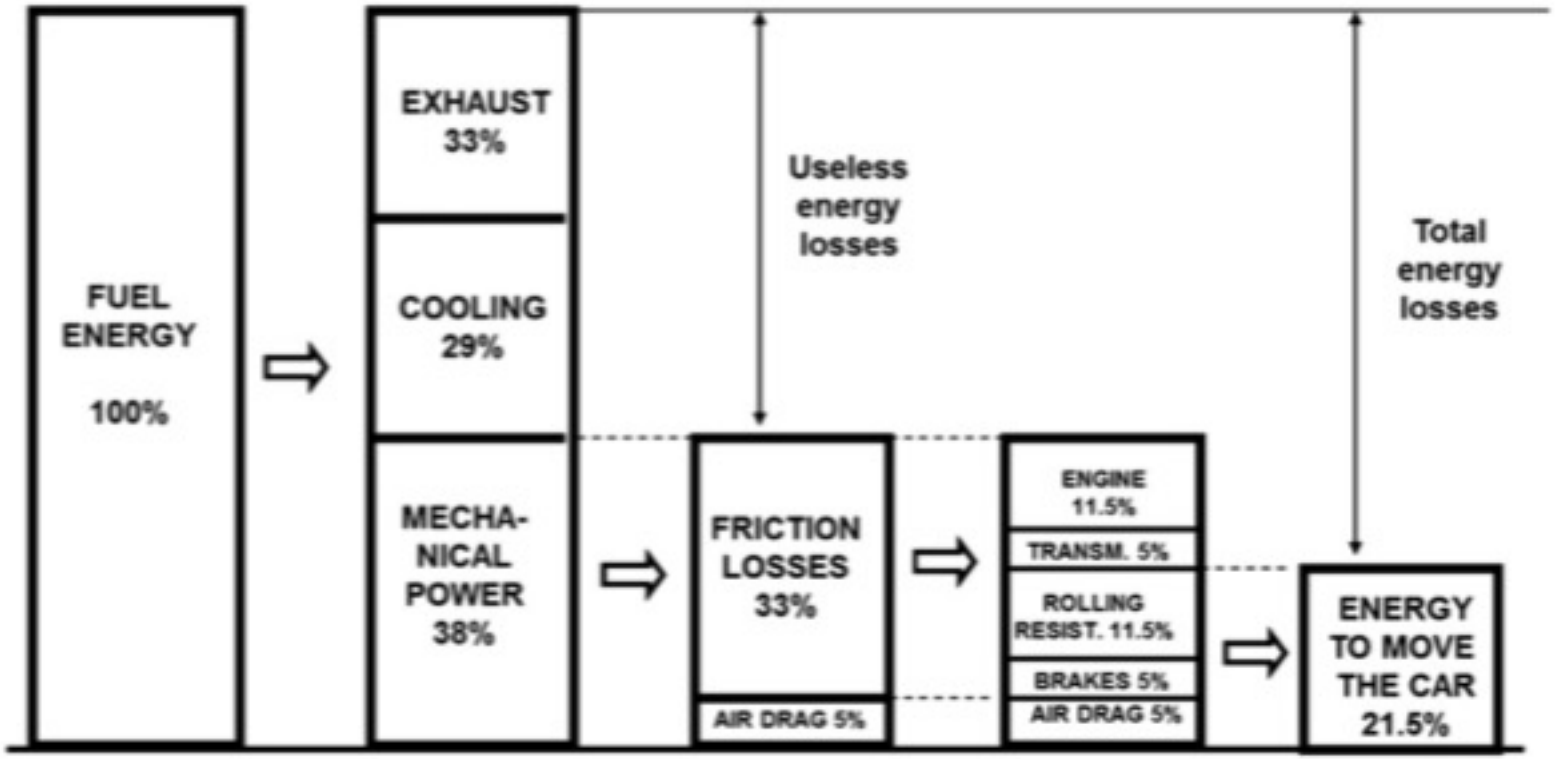

Fig. 4. Breakdown of passenger car energy consumption.

Solid lubricant thin films

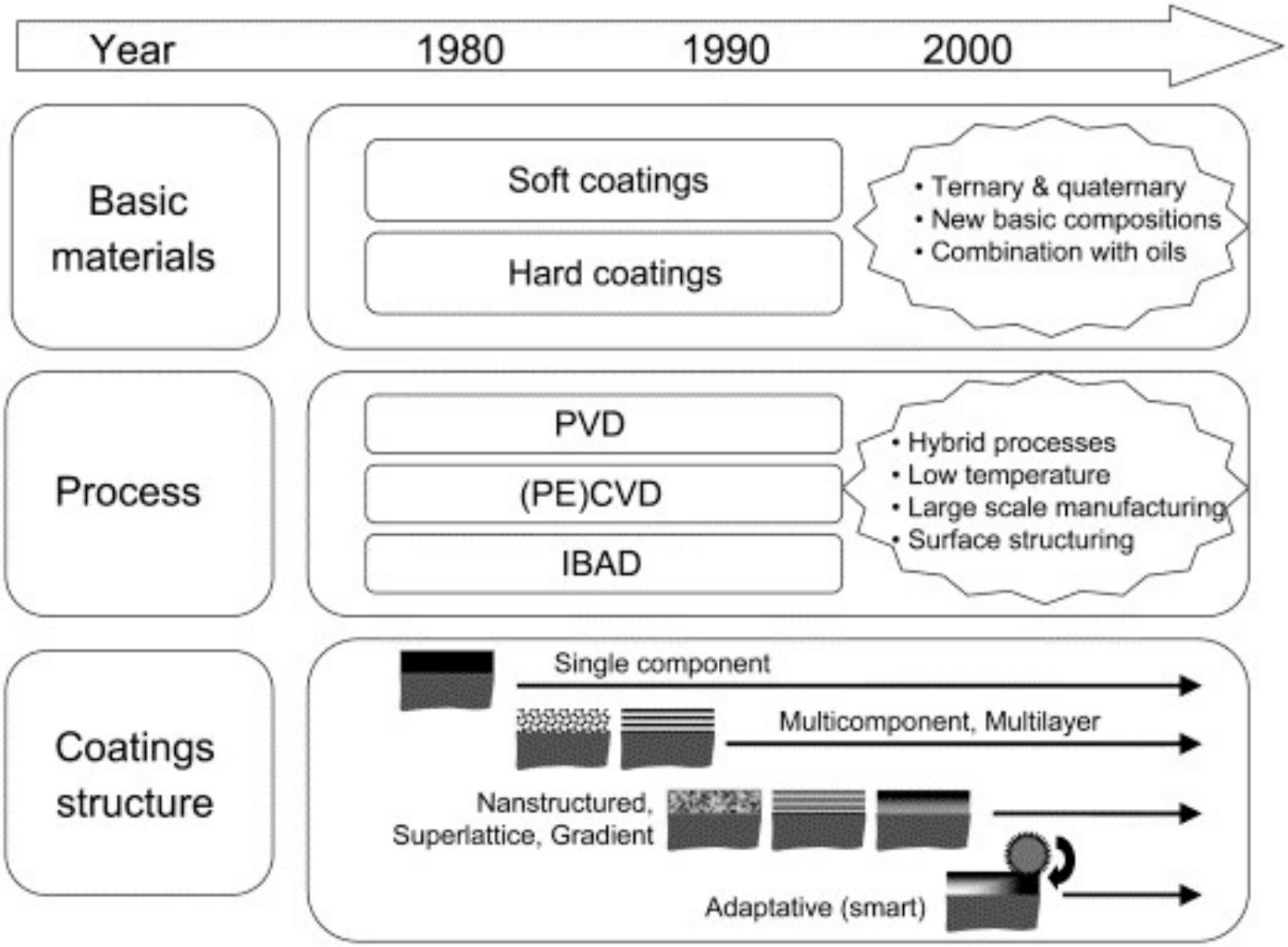

Donnet, Erdemir, Surface and Coatings Technology Volumes 180–181, 1 March 2004, Pages 76–84

Hard coatings Hardness higher than ≈ 10 GPa	Soft coatings Hardness lower than ≈ 10 GPa
Nitrides TiN, CrN, ZrN, BN, $BaSO_4$	**Soft metals** Ag, Pb, Au, In, Sn, Cr, Ni, Cu
Carbides TiC, WC, CrC	**Lamellar solids** MoS_2, WS_2, Graphite H_3BO_3, HBN, GaS, GaSe
Oxides Al_2O_3, Cr_2O_3, TiO_2, ZnO, CdO, Cs_2O, PbO, Re_2O_7	**Halides sulfates, sulfur** CaF_2, BaF_2, PbS, $CaSO_4$, $BaSO_4$
Borides TiB_2	**Polymers** PTFE, PE, Polyimide Polymerlike DLC
DLC & Diamond a-C, ta-C, a-C:H, ta-C:H, CN_x a-C:X(:H), (nc-)diamond	

DLC = diamondlike carbon
a= amorphous
ta = tetrahedral amorphous
X = a metal
nc = nanocrystalline
PTFE = polytetrafluorethylene
PE = polyethylene

Figure 2. Classification of tribological coatings, depending on the nature of the constituting material.

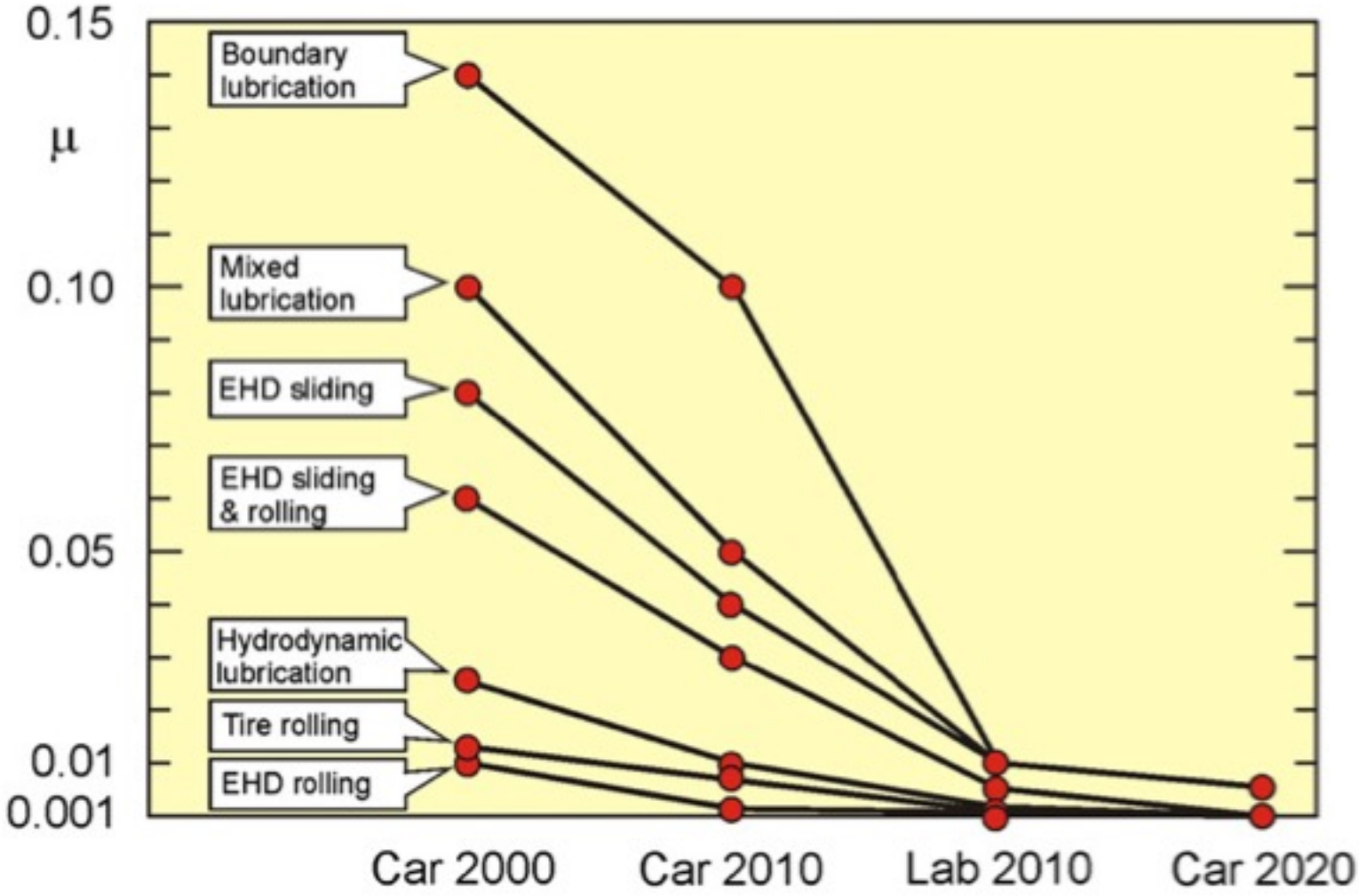

Fig. 5. Trends in the reductions in coefficients of friction in the four passenger car categories for different lubrication mechanisms and for rolling friction.

Decorative coatings PACVD on plastic

https://www.oerlikon.com/balzers/com

Title

https://www.oerlikon.com/balzers/com

Decorative DLC and other PVD from DIARC Ltd

Architectural, Automotive Glass & WEB Coating

http://www.testbourne.com/architectural-automotive-glass-web-coating

Roll to Roll for decorative and gas barrier

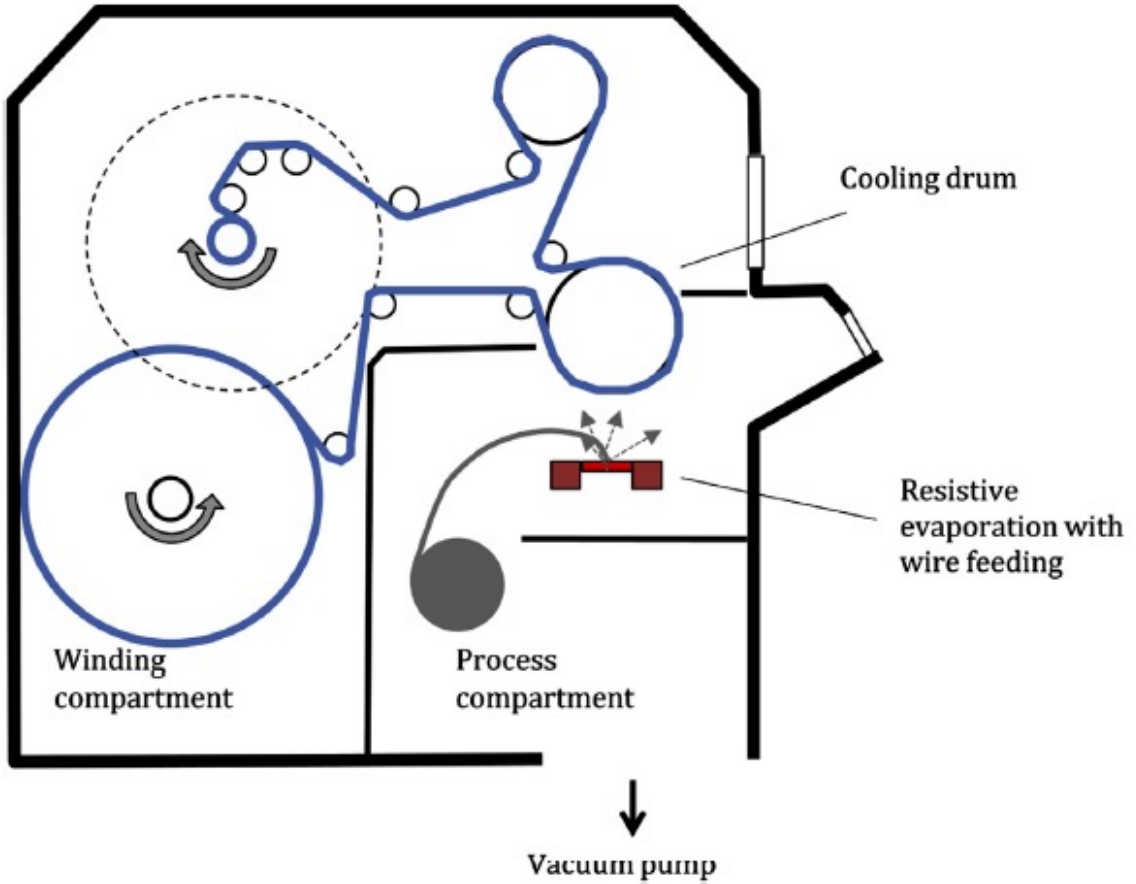

Figure 6 Schematic illustration of a web-coating device with thermal evaporation. After Ludwig, R.; Kukla, R.; & Josephson, E. Vacuum Web Coating – State of the Art and Potential for Electronics. *Proc. IEEE* **2005**, *93* (8), 1483–1490.

Figure 7 Array of aluminum evaporation. With permission of Leybold Optics GmbH.

Permeation

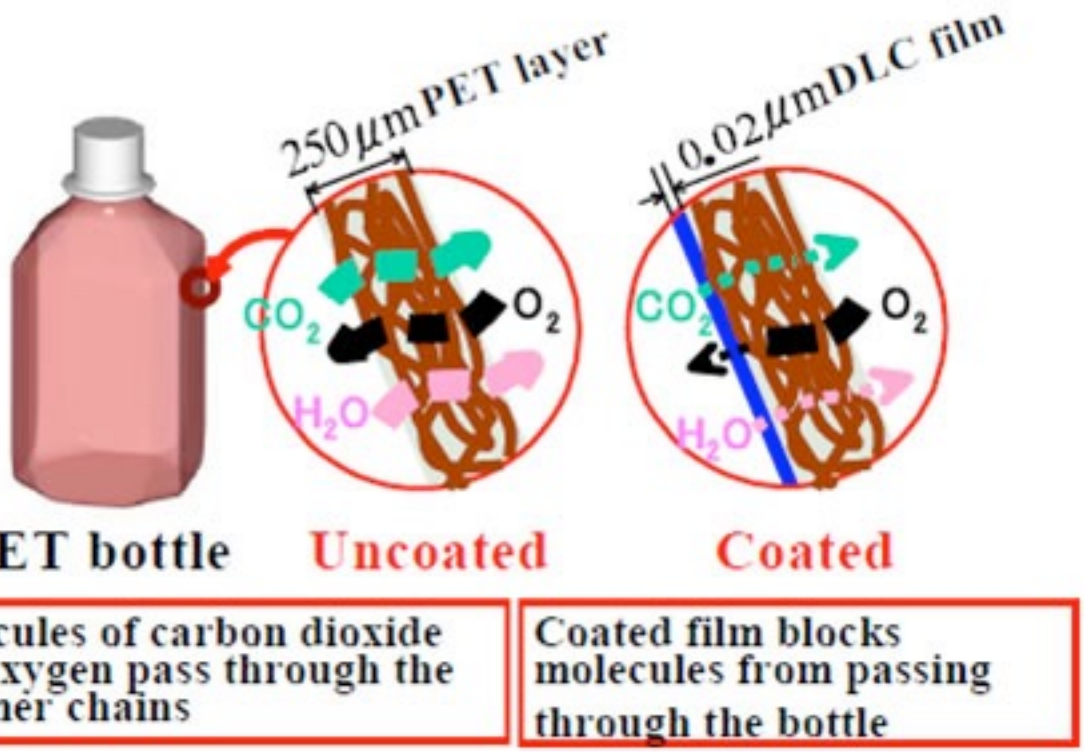
250μm PET layer
0.02μm DLC film
CO2
O2
H2O
CO2
O2
H2O
PET bottle
Uncoated
Coated
Molecules of carbon dioxide and oxygen pass through the polymer chains
Coated film blocks molecules from passing through the bottle

Title

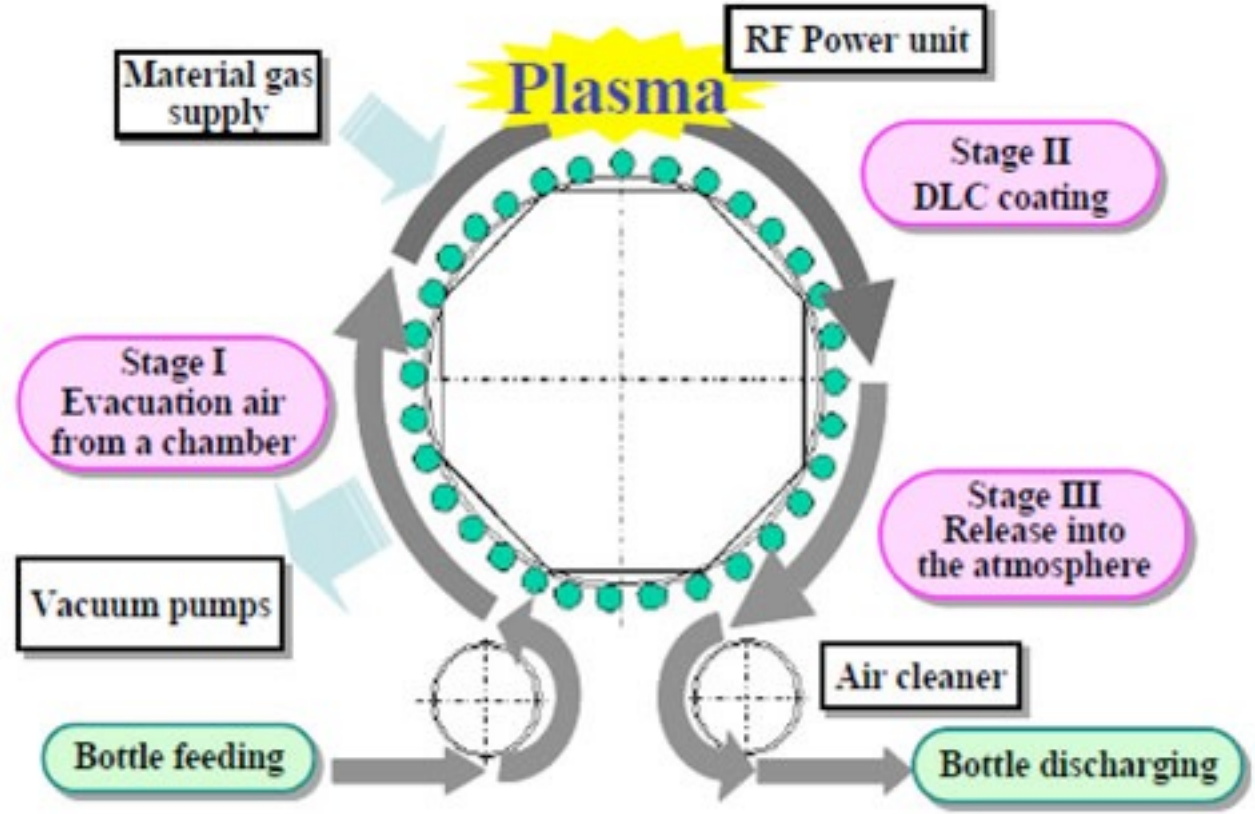
RF Power unit
Material gas supply
Plasma
Stage II
DLC coating
Stage I
Evacuation air from a chamber
Stage III
Release into the atmosphere
Vacuum pumps
Air cleaner
Bottle feeding
Bottle discharging

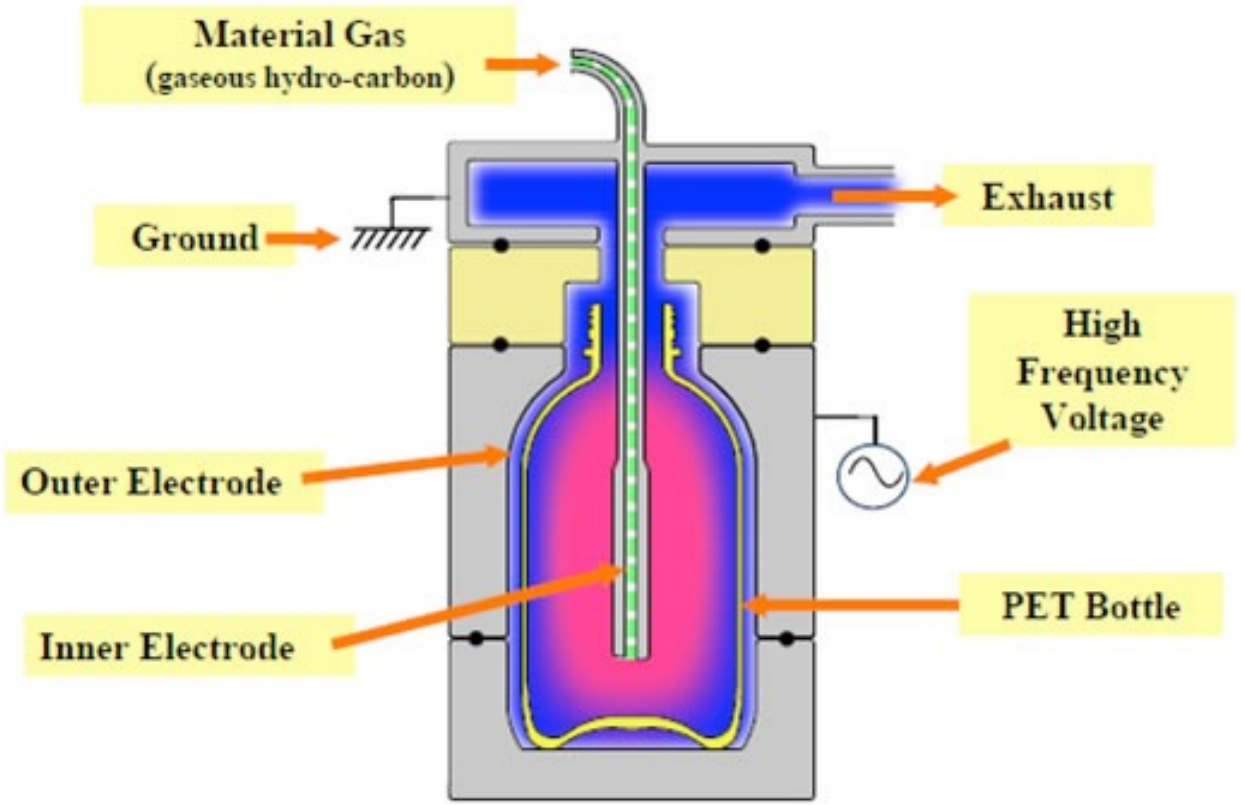
Material Gas
(gaseous hydro-carbon)
Exhaust
Ground
High
Frequency
Voltage
Outer Electrode
PET Bottle
Inner Electrode

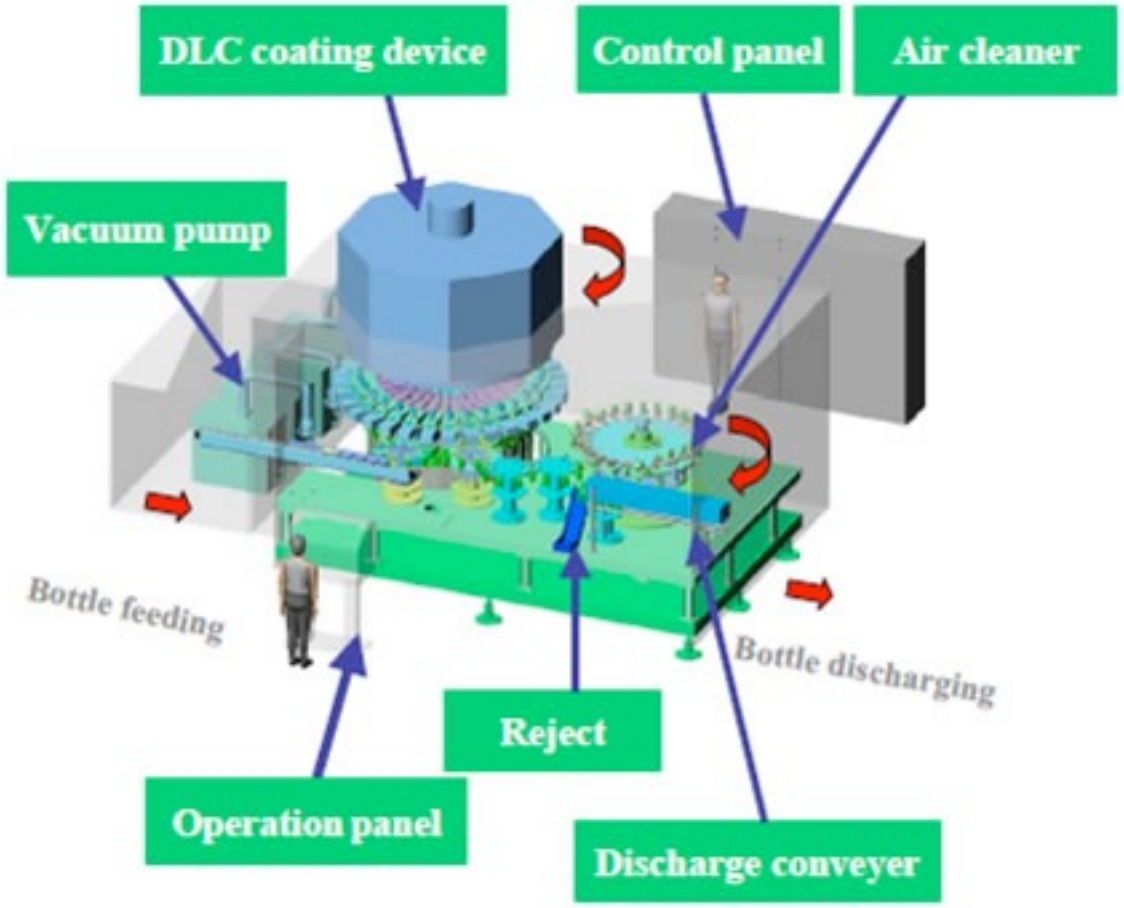
DLC coating device
Control panel
Air cleaner
Vacuum pump
Bottle feeding
Bottle discharging
Reject
Operation panel
Discharge conveyer

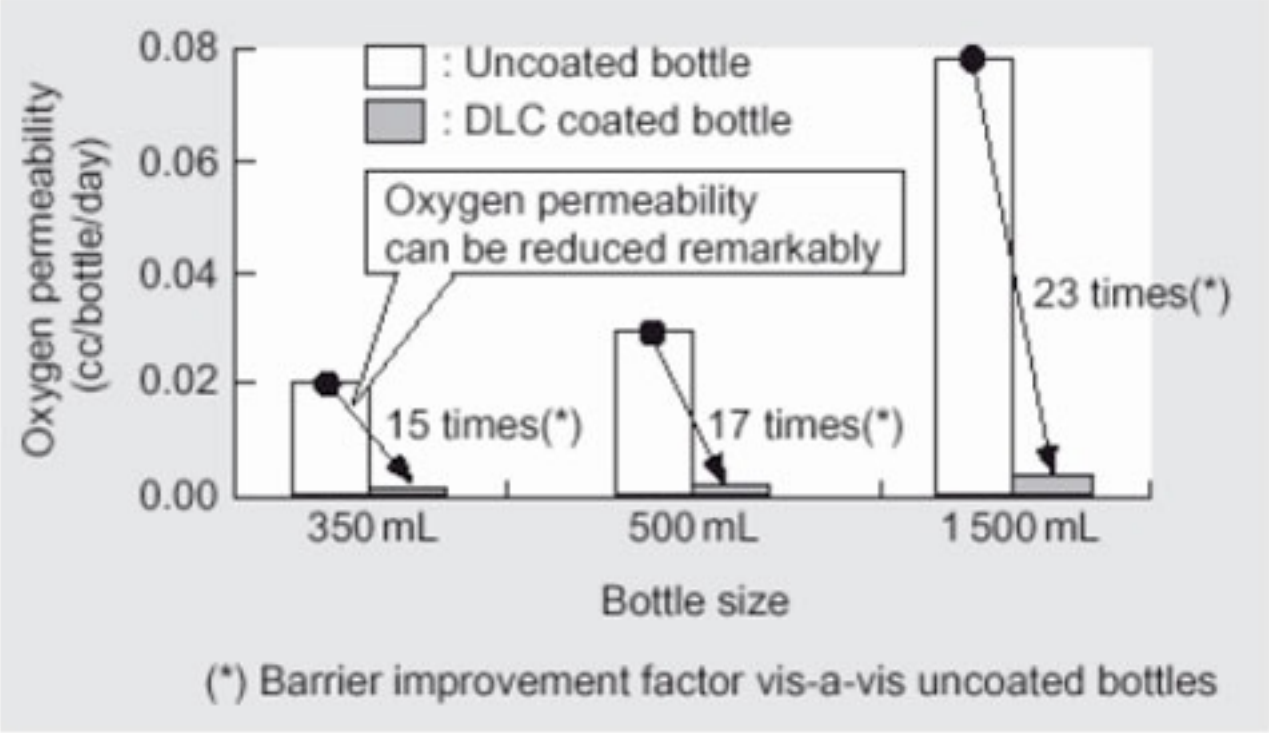
Oxygen permeability (cc/bottle/day)
0.08
0.06
0.04
0.02
0.00
: Uncoated bottle
: DLC coated bottle
Oxygen permeability can be reduced remarkably
15 times(*)
17 times(*)
23 times(*)
350 mL
500 mL
1 500 mL
Bottle size
(*) Barrier improvement factor vis-a-vis uncoated bottles

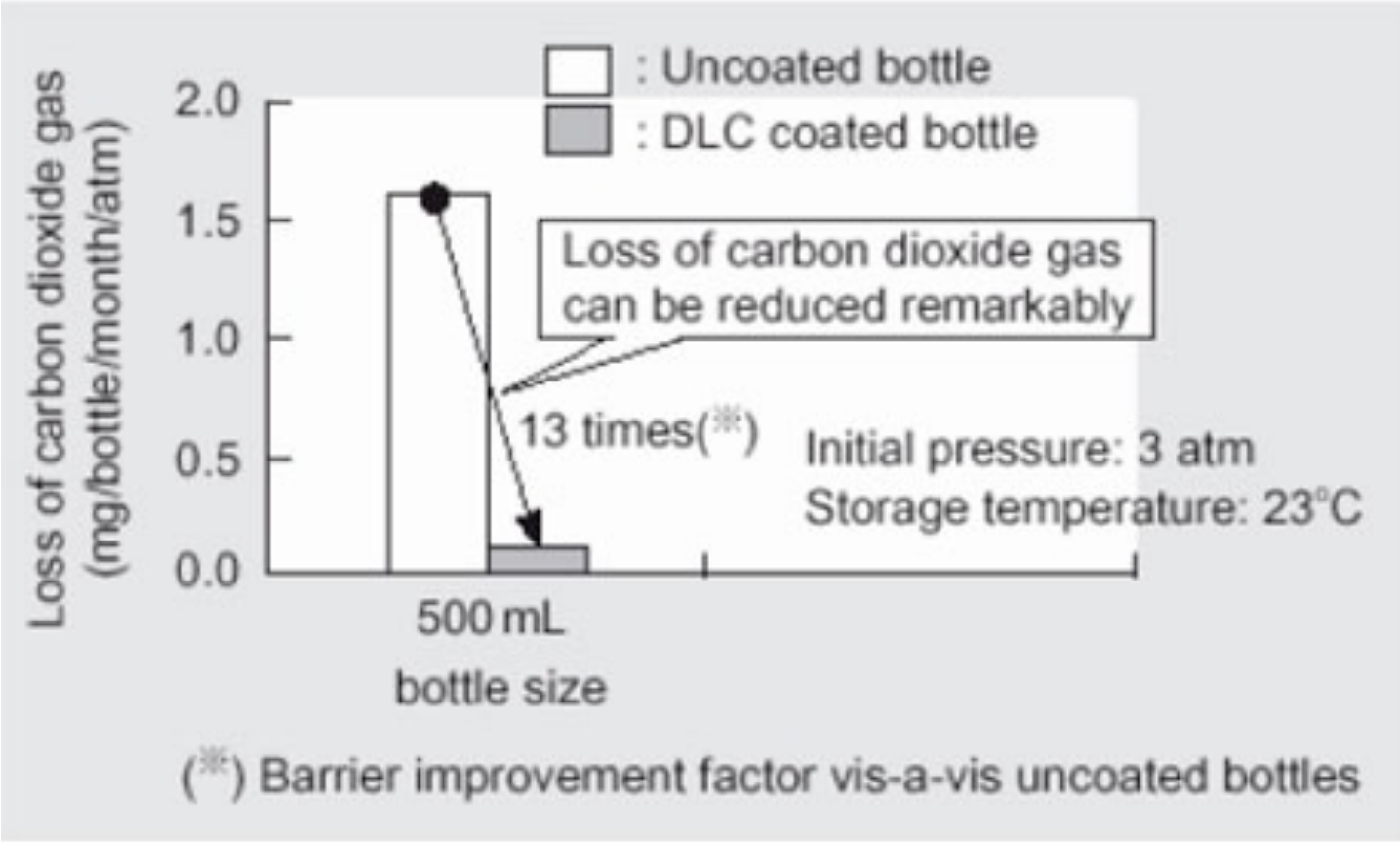
: Uncoated bottle
: DLC coated bottle
Loss of carbon dioxide gas
(mg/bottle/month/atm)
2.0
1.5
1.0
0.5
0.0
Loss of carbon dioxide gas
can be reduced remarkably
13 times(※)
Initial pressure: 3 atm
Storage temperature: 23°C
500 mL
bottle size
(※) Barrier improvement factor vis-a-vis uncoated bottles

ALD barrier for OLED on polymer web

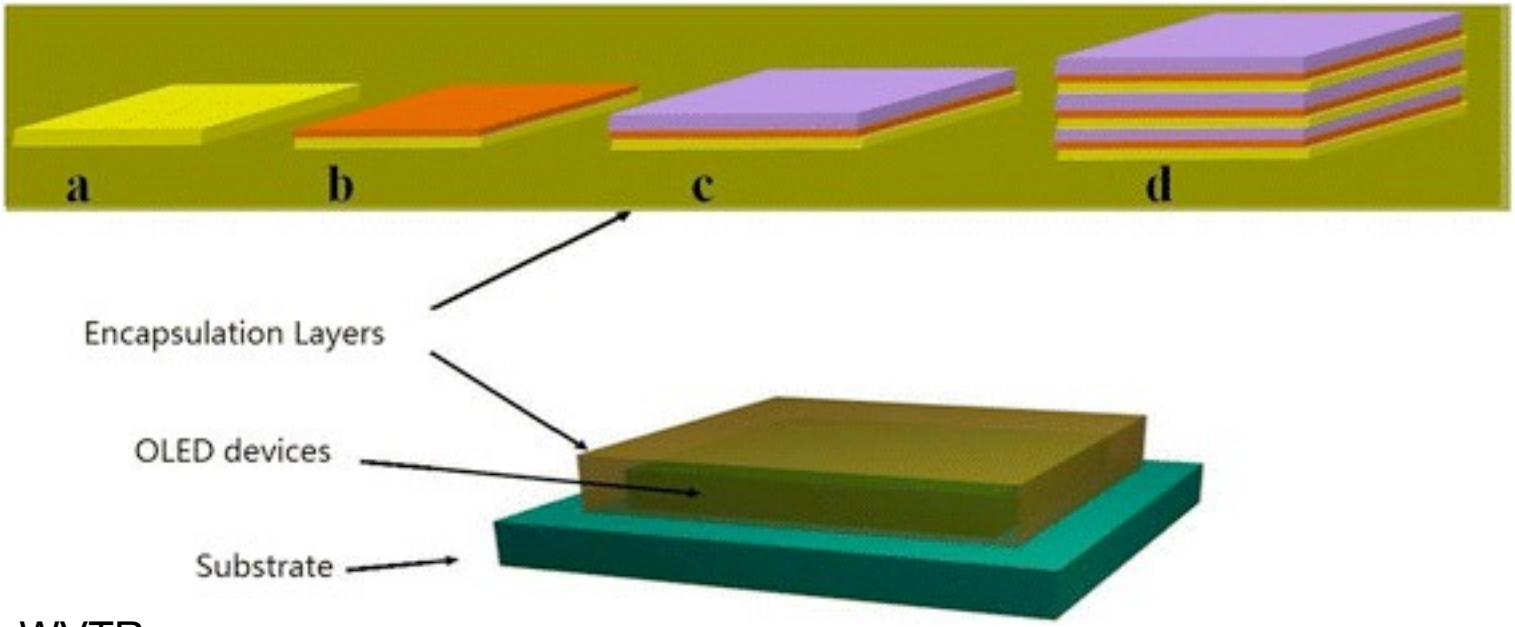

WVTR:

- 8.5 × 10−5 g/m^2/day at 25°C, 85% RH
- half lifetime 380 h luminance 1,500 cd/m^2 for a green organic light-emitting diode

Hao Zhang et al., Nanoscale Research Letters 2015,10:169

ALD for encapsulation

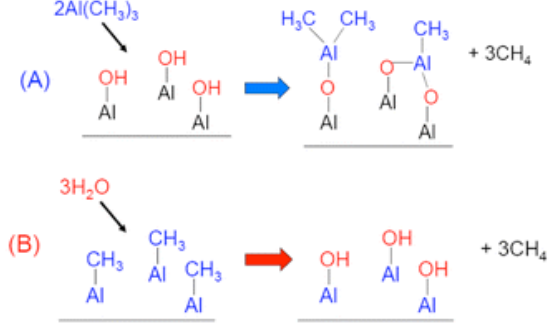

(a) The reaction of ALD processes for Al_2O_3 film

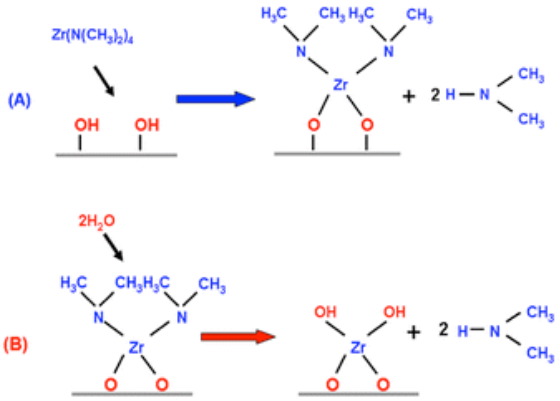

(b) The reaction of ALD processes for ZrO_2 film

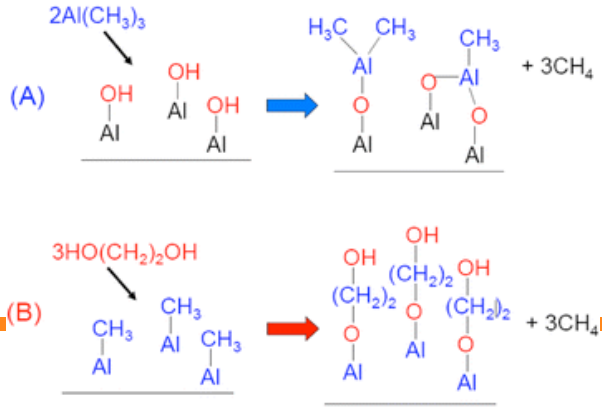

(c) The reaction of MLD processes for alucone film

Aalto University
School of Chemical Technology

Hao Zhang et al., Nanoscale Research Letters 2015,10:169

Corrosion resistance

G. Wu et al. , Materials Letters, Volume 62, Issue 28, 15 November 2008, Pages 4325–4327

AlZ31 (Mg + Al 3wt%. Zn 1wt%) with MS Al 250nm

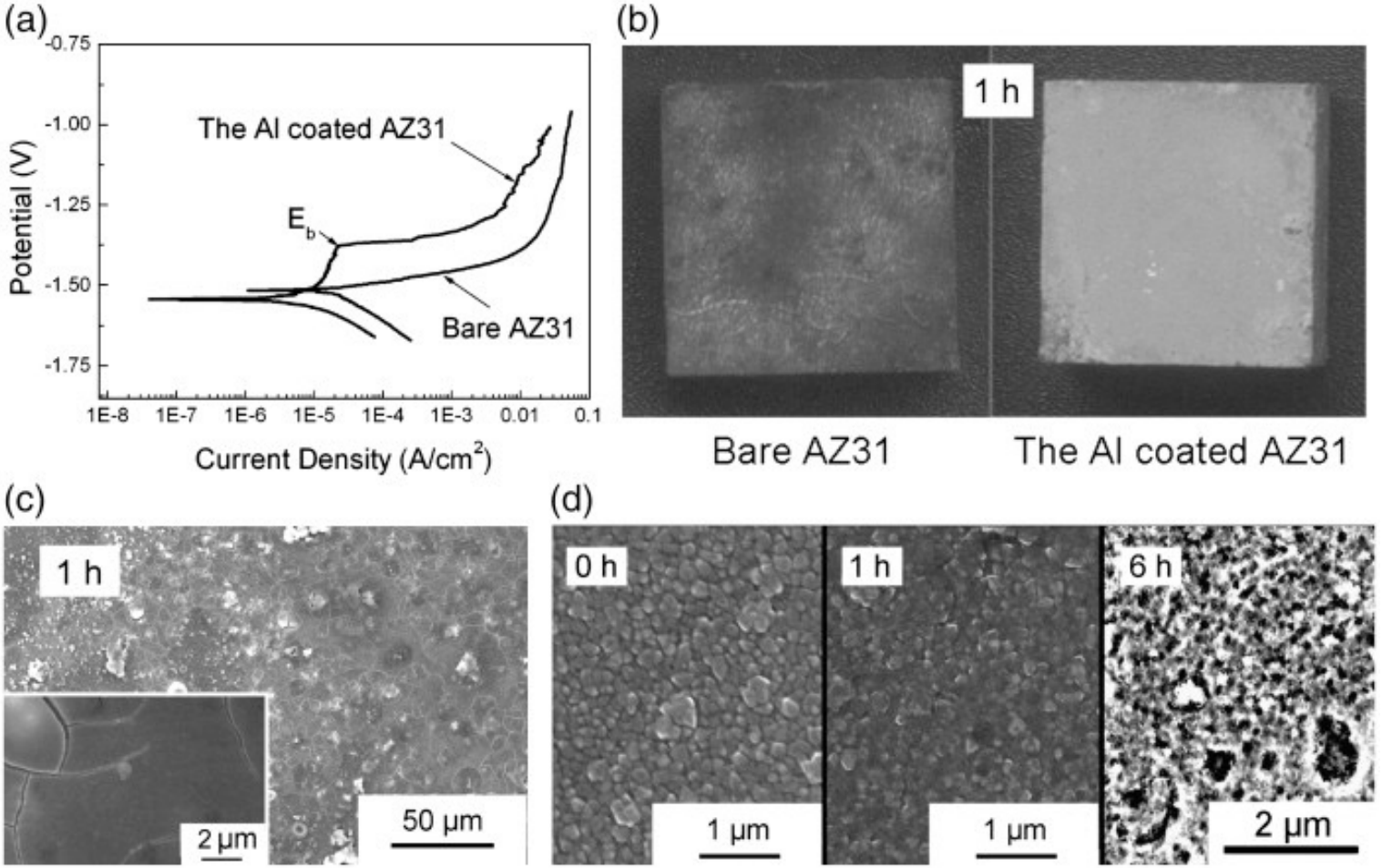

Fig. 2.

(a) Polarization curves of the coated AZ31 and bare AZ31. (b) Appearance of the samples after 1 h of immersion. (c) Surface morphology of the Al coated AZ31 observed by SEM after 1 h of immersion. The insert shows the morphology of the cracks. (d) Surface morphologies of the Al coated AZ31 observed by FESEM at a higher magnification after different immersion time (0 h, 1 h and 6 h).

Multilayer PVD MS CrN + ALD nanolaminate

- MS of Cr (Commercial Balinit CNI) 3 µm + ALD Al_2O_3/TiO_2 nanolaminate 50 nm

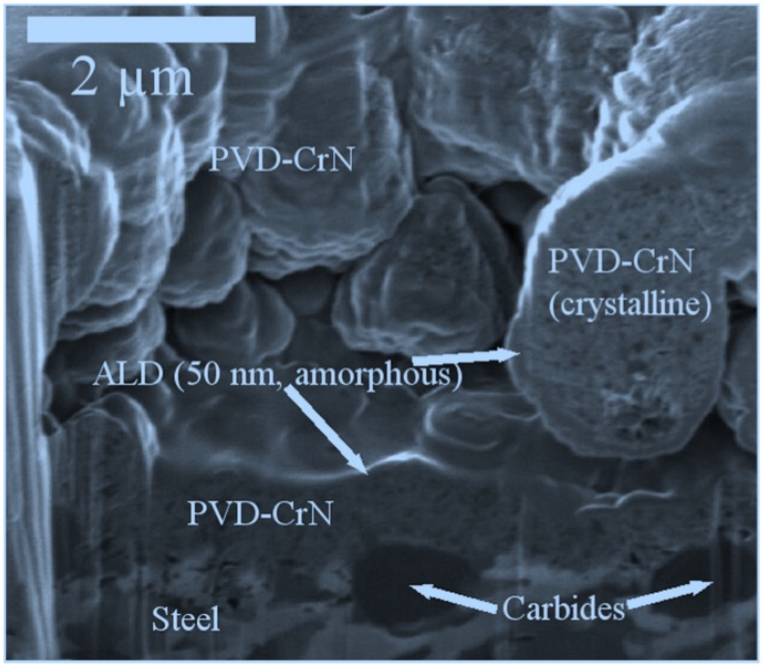

Fig. 10. Cross-sectional image taken from CrN pinhole, from the multilayer PVD/ALD nanolaminate sample (*default*).

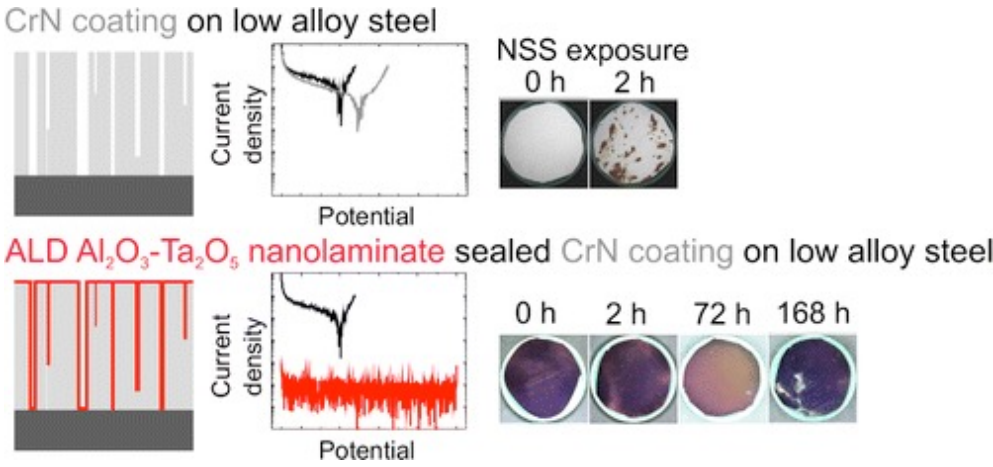

Sealing of hard CrN and DLC coatings with atomic layer deposition
E Härkönen, I Kolev, B Díaz… - … applied materials & …, 2014 - ACS Publications

Leppäniemi, J. et al., 2017. Thin Solid Films. *Thin Solid Films*, 627, pp.59–68.

Leppäniemi, J. et al., 2017. Thin Solid Films. *Thin Solid Films*, 627, pp.59–68.

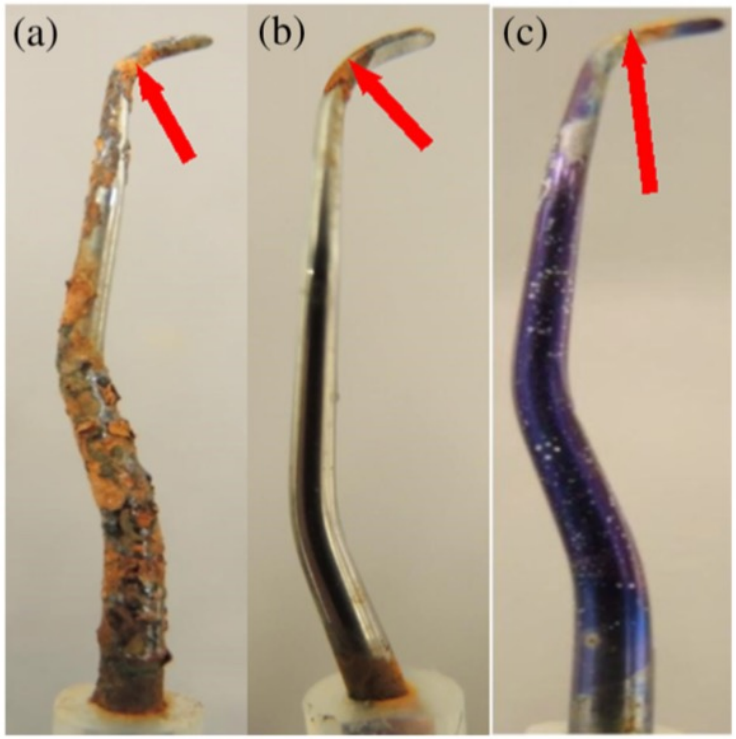

Fig. 9. HSS dental curettes after 48 h in NSS testing: a) non-coated b) CrN coated c) CrN/ALD-nanolaminate (default). Arrow denotes lateral surface of the curette, where the surface roughness of the tool is higher.